Variability of the Tropical Ocean Surface Temperatures at Decadal–Multidecadal Timescales. Part I: The Atlantic Ocean

VIKRAM M. MEHTA

NASA–University of Maryland Joint Center for Earth System Science, Department of Meteorology, University of Maryland, College Park, Maryland

(Manuscript received 11 December 1996, in final form 8 October 1997)

ABSTRACT

Gridded time series from the *Global Ocean Surface Temperature Atlas* were analyzed with a variety of techniques to identify spatial structures and oscillation periods of the tropical Atlantic sea surface temperature (SST) variations at decadal timescales, and to develop physical interpretations of statistical patterns of decadal SST variations. Each time series was 110 yr (1882–1991) long. The tropical Atlantic SST variations were compared with decadal variations in a 74-yr-long (1912–85) north Nordeste Brazil rainfall time series and a 106-yr-long (1886–1991) tropical Atlantic cyclone activity index time series. The tropical Atlantic SST variations were also compared with decadal variations in the extratropical Atlantic SST.

Multiyear to multidecadal variations in the cross-equatorial dipole pattern identified as a dominant empirical pattern of the tropical Atlantic SST variations in earlier and present studies are shown to be variations in the approximately north–south gradient of SST anomalies. It is also shown that there was no dynamical–thermodynamical, dipole mode of SST variations during the analysis period. There was a distinct decadal timescale (12–13 yr) of SST variations in the tropical South Atlantic, whereas no distinct decadal timescale was found in the tropical North Atlantic SST variations. Approximately 80% of the coherent decadal variance in the cross-equatorial SST gradient was ''explained'' by coherent decadal oscillations in the tropical South Atlantic SSTs. There were three, possibly physical, modes of decadal variations in the tropical Atlantic SSTs during the analysis period. In the more energetic mode of the North Atlantic decadal SST variations, anomalies traveled into the tropical North Atlantic from the extratropical North Atlantic along the eastern boundary of the basin. The anomalies strengthened and resided in the tropical North Atlantic for several years, then frequently traveled northward into the mid–high-latitude North Atlantic along the western boundary of the basin, and completed a clockwise rotation around the North Atlantic basin. In the less energetic North Atlantic decadal mode, SST anomalies originated in the tropical–subtropical North Atlantic near the African coast, and traveled northwestward and southward. In the South Atlantic decadal SST mode, anomalies either developed in situ or traveled into the tropical South Atlantic from the subtropical South Atlantic along the eastern boundary of the basin. The anomalies strengthened and resided in the tropical South Atlantic for several years, then frequently traveled southward into the subtropical South Atlantic along the western boundary of the basin, and completed a counterclockwise rotation around the South Atlantic basin. These decadal modes were not a permanent feature of the tropical Atlantic SST variations. The tropical North and South Atlantic SST anomalies frequently extended across the equator. Uncorrelated alignments of decadal SST anomalies having opposite signs on two sides of the equator occasionally created the apperance of a dipole.

Independent analyses of the north Nordeste Brazil rainfall showed physical consistency and high coherence with the cross-equatorial SST gradient oscillations at 12–13-yr period. The tropical Atlantic cyclone index showed physical consistency but moderate coherence with the tropical North Atlantic decadal SST variations. The quasi-regularity of the 12–13-yr oscillations in the cross-equatorial SST gradient may provide an opportunity for long lead-time, skillful predictions of climate anomalies in the tropical Atlantic sector.

1. Introduction

Natural variability of the climate system at decadal (8–20 yr) to multidecadal timescales has received increased attention over the last two decades. It is important to study this natural variability to see if it is predictable and for its potential to interact with anthropogenic climate change.

Inadequate spatial coverage of long (~100 yr) observational records containing reliable measurements hampers any observational study seeking to characterize decadal timescale climate variability. This is especially true in tropical regions. Since shipboard measurements were the primary source of information about sea surface temperature (SST) until the advent of earth-orbiting satellites, spatial coverage of long observational records containing reliable measurements is dependent upon and limited by locations of shipping routes. The present

Corresponding author address: Dr. Vikram M. Mehta, Joint Center for Earth System Science, University of Maryland, Department of Meteorology, College Park, MD 20742.
E-mail: mehta@atmos.umd.edu

work is an attempt to characterize decadal variations of the tropical Atlantic SSTs using shipboard measurements compiled by Bottomley et al. (1990) in the *Global Ocean Surface Temperature Atlas* (GOSTA). Decadal variations of the GOSTA SSTs in the tropical Pacific and Indian Oceans will be described in Part II.

Previous work on the analysis of tropical Atlantic SST variations is reviewed briefly in section 2, brief descriptions of the data are given in section 3, and data analysis techniques are described in section 4. Results of the analyses are described in sections 5 and 6. Concluding remarks are presented in section 7.

2. Review of previous work

In studying variability of the coupled ocean–atmosphere system, the Atlantic region has been the subject of numerous studies, primarily because of the availability of relatively long observational records of various climate quantities. Until recently, only a few decades long record of SST, however, was available at relatively high spatial resolution covering extensive areas of the tropical Atlantic Ocean. Mehta and Delworth (1995, hereafter referred to as MD), and Enfield and Mayer (1997) have reviewed the results of analyses of these relatively short SST time series. Variations of other climate quantities in the tropical Atlantic region have been associated with multiyear SST variations. Folland et al. (1986, 1991), Semazzi et al. (1988), Hastenrath (1990), and Ward and Folland (1991), among others, have found correlations between African rainfall variations and the tropical Atlantic SST variations. Numerous studies (see, e.g., Hastenrath 1991; Nobre and Shukla 1996, and references therein) have found correlations among variations in the tropical Atlantic SST, atmospheric circulation over the tropical Atlantic, and rainfall over northeast Brazil at multiyear timescales.

In these analyses of relatively short SST time series on a regular spatial grid, the pattern of multiyear variations that has attracted the most attention has nearly constant amplitude with respect to longitude in the tropical Atlantic and opposite signs on the two sides of the equator, with the maximum amplitudes at approximately 15°N and 15°S latitude. This north–south, cross-equatorial pattern results from empirical orthogonal function (EOF) analysis of tropical Atlantic SST anomalies and has been characterized by some researchers as a dipole mode of tropical Atlantic SST variability. This type of SST pattern also emerges when wind or rainfall anomalies over the tropical Atlantic and some neighboring continental regions are regressed against SST anomalies. Houghton and Tourre (1992), however, questioned the physical interpretation of the dipole and used rotated EOF (REOF) analysis to show that SSTs in the tropical Atlantic undergo independent interannual variations on the two sides of the equator. Kawamura (1994) calculated REOFs of global, monthly average SST anomalies in 5° lat × 5° long grid boxes during the 34-yr period from January 1955 to December 1988. Spatial patterns of his REOFs 3 and 4 show SST variations confined largely to the North Atlantic and to the South Atlantic, respectively. Neither of these REOF patterns shows dipolelike, cross-equatorial, interannual SST variations. The recent analysis of SST and other data derived from the Comprehensive Ocean–Atmosphere Data Set by Enfield and Mayer (1997) has also confirmed this result.

Using 11 time series, each 100 yr long, from an earlier version of the GOSTA dataset, MD analyzed decadal variations of the tropical Atlantic SSTs. A variety of analyses of the GOSTA time series suggested that there were two types of pronounced, quasi-oscillatory, decadal timescale SST variations in the tropical Atlantic region. One type, characterized by timescales between approximately 8 and 11 yr, had high spatial coherence within each tropical Atlantic hemisphere but not between the two hemispheres. The second type, characterized by periods between 12 and 20 yr, had high spatial coherence between the two hemispheres and was considerably weaker than the first.

In many of the earlier studies, the EOF analysis was used to diagnose variations in the tropical Atlantic SSTs and some of the dominant EOF patterns were interpreted as dynamical modes of variations of the tropical Atlantic SSTs. It is well known (see, e.g., Horel 1981), however, that despite its ability to reduce the number of degrees of freedom of a large dataset into a relatively few energetic patterns of variations, spatial orthogonality of the eigenvectors is a strong constraint imposed on the resulting empirical patterns. Once the pattern containing the most variance is determined by the EOF analysis technique, the subsequent patterns are often predictable because of the orthogonality constraint. This constraint is also responsible for the dependence of the empirical patterns on the geographical domain of the EOF analysis. Linearly combining a few EOF patterns into REOFs (see, e.g., Horel 1981, and references therein) alleviates some of these problems but the phase difference between coefficients within an EOF pattern can only be either 0° or 180°, forcing individual EOF patterns (simple or rotated) to contain only standing oscillations. Complex EOF analysis (Rasmusson et al. 1981; Barnett 1983; Horel 1984) can reveal stationary and traveling variations in the same empirical pattern, but the patterns in these three types of EOF analysis are obtained statistically and are not required to have any dynamical significance. There have been attempts to link EOFs and physical modes of variability in some cases such as linear dynamical systems with normal modes satisfying a self-adjoint equation (North 1984) and shallow water equations (Brunet and Vautard 1996), but it is not clear that any one statistical analysis can reveal patterns of climate variations that are also dynamically significant. Therefore, several other techniques, besides these three types of EOF analysis, were used in the present study to develop physical interpretations of statistical patterns.

Even though the earlier studies yielded interesting indications of SST variations at periods longer than a few years, these studies were handicapped by the availability of relatively long SST time series only in a few regions or relatively short time series over the entire tropical Atlantic Ocean. Therefore, spatial patterns of decadal variations were not analyzed and the presence or absence of distinctness of decadal timescales was not established. Another drawback of the previous studies was that the possibility of relationships between SST variations in the tropical and mid–high-latitude parts of the Atlantic Ocean at decadal timescales was not explored. More importantly, it was not clear from the earlier studies whether the empirical patterns of SST variations were also physical modes of tropical Atlantic SST variability. Therefore, the present study was designed to assemble the maximum possible number of long, usable SST time series; to include the Atlantic Ocean from 40°S to 60°N in this study; to develop, if possible, physical interpretations of dominant empirical patterns; and to identify physical modes of SST variations if there are any. Seventy time series, each 110 yr long and 38 of them between 30°S and 30°N, were extracted from the GOSTA and were analyzed with a variety of techniques. Decadal variations in the tropical Atlantic SST anomalies were also compared with decadal variations in the north Nordeste Brazil rainfall and an index of the tropical Atlantic cyclone activity. Specifically, the following questions were addressed to these datasets. Are there distinct decadal periods at which the tropical Atlantic SSTs oscillate? Are there large-scale, spatially coherent structures of the tropical Atlantic SST anomalies that oscillate at decadal periods? Is there a definite relationship between the tropical Atlantic and mid-high latitude Atlantic SST variations? Are there identifiable physical modes of decadal SST variations? Is there covariability among the SSTs, the north Nordeste Brazil rainfall, and the tropical Atlantic cyclone index at decadal timescales?

3. The datasets

a. The GOSTA SST measurements

The GOSTA has been compiled by Bottomley et al. (1990) from ship observations. The MOHSST5 version of the GOSTA SST data was used in the present study. Parker et al. (1994) have described the data quality checks incorporated in the MOHSST5 version. The monthly average SST anomalies since 1856 (with respect to the 1951–80 climatology of each time series) are available on a regular, global, 5° lat × 5° long grid. The number of measurements, however, is not uniform in time. Shipping routes in the tropical Atlantic Ocean were relatively well developed since the last quarter of the nineteenth century, but the time series of monthly data in 5° lat × 5° long grid boxes are not continuous. Since one of the major goals of this work was to identify spatial structures of decadal variations, the spatial and temporal coverages of the SST anomalies were maximized by averaging in space and time.

Following MD, monthly anomalies were averaged to form annual anomalies subject to the criterion that four or more monthly observations be available for each year. The years in which this criterion was not satisfied were regarded as not having any data. Folland et al. (1993) compared six operational SST analyses and recommended that 10° lat × 10° long areas may have reasonable data coherence for the analysis of shipboard measurements in the tropical South Atlantic Ocean. Therefore, after the annual averaging, time series from four adjacent grid boxes were averaged (the four grid boxes represent an area of approximately one million square kilometers). For years in which none of the four grid boxes had observations, an SST anomaly value was assigned by linear interpolation from adjacent years. The maximum number of consecutive missing points allowed was four. The missing data were linearly interpolated. Over the Atlantic Ocean between 40°S and 60°N (both latitudes outer boundaries of grid boxes), usable SST anomalies for the period 1882 to 1991 were assembled. Enough observations were found to assemble annual-average time series over 38 such nonoverlapping 10° lat × 10° long grid boxes between 30°S and 30°N. The tropical Atlantic in this study denotes the region from 30°S to 30°N since each grid box covers 10° lat. Seventy such time series were formed over the Atlantic Ocean from 40°S to 60°N.

Since measurement techniques have changed over the analysis period, estimated corrections to the measured SST are also available in the same dataset. The corrected SST time series were used in the present work because MD found that the corrections applied for changes in measurement techniques apparently preserved the basic spectral characteristics of the 11 time series analyzed by them.

b. The north Nordeste Brazil rainfall

Ward and Folland (1991) have combined normalized rainfall anomaly time series over north Nordeste Brazil from two sources. One source is C. Nobre's February–May north Nordeste rainfall for 1912–81 (Ward and Folland 1991) and the other source is Hastenrath et al.'s (1984) March–April north Nordeste rainfall for 1982–85. The combined normalized rainfall anomaly time series from 1912 to 1985 was used in the present study.

c. The tropical Atlantic cyclone activity index

Gray et al. (1992, 1994) and Landsea (1993) have combined six measures of seasonal tropical Atlantic cyclone activity into an index of net tropical cyclone (NTC) activity. The six measures are the seasonal total numbers of named storms, hurricanes, intense hurricanes, named storm days, hurricane days, and intense

hurricane days. The NTC index is an arithmatic average of the percentage departure of each of the measures from their respective long-term averages. The NTC index for the Atlantic basin from 1886 to 1991 was used in the present study. The NTC index before the mid-1940s is not reliable (Landsea 1993) because of changes in observation platforms/techniques.

4. Analysis techniques

A variety of time series analysis techniques were used to characterize decadal variations in the tropical Atlantic SSTs, and their association with variations in extratropical Atlantic SSTs, the north Nordeste Brazil rainfall, and the tropical Atlantic cyclone activity.

a. Spectrum analysis

The Fourier spectrum analysis (FSA), based on the fast Fourier transform technique, was used to estimate spectra of time series. Each spectral estimate shown in this paper has approximately five degrees of freedom. Preliminary results shown in MD suggested the presence of distinct decadal timescales, therefore a priori significance tests of spectral peaks were used in the present study. The statistical significance of spectral peaks was tested with a Monte Carlo simulation technique (Press et al. 1987). It was hypothesized that the time series, whose spectral peaks were to be tested, was one realization of a ''red noise'' process and that the peaks occurred due to sampling errors and a relatively short length of the time series. If there were many realizations of the red noise process, it would be possible to quantify the range of spectral densities and the number of peaks that might occur due to these problems at each Fourier frequency. Therefore, 10 000 realizations of the red noise process were simulated. Each realization had the same length, lag-one autocorrelation, and variance as the original time series. The Fourier spectrum of each simulated time series was estimated and the spectral density at or below which 95% of the 10 000 spectral densities at each frequency lay was found. Thus, there would be only 5% probability of a peak in the spectrum of the original time series exceeding this limit due to chance. The number of spectral peaks at each frequency in the entire 10 000-spectra ensemble was also found.

Cross-spectra between pairs of time series were estimated from the Fourier transforms of the cross-covariance function of the two time series. Squared coherence and phase difference between the two time series at each Fourier frequency were then calculated from the spectra and cross-spectra of the two time series. The 95% and 99% confidence levels on the squared coherence were calculated using the formula developed by Bloomfield (1976).

The singular spectrum analysis (SSA; Broomhead and King 1986; Vautard and Ghil 1989; Penland et al. 1991; MD) was used to verify and complement the results obtained with the FSA. Since the EOFs and the principal components (PCs) in the SSA are functions of time, they are usually referred to as T-EOFs and T-PCs, respectively. The T-EOFs and T-PCs can be combined to reconstruct any subset of components of the original time series. Thus, application of the SSA yields data-adaptive coherent structures as in space–time EOF analysis. A pair of quasi-oscillatory T-EOFs in quadrature, with relatively large and approximately equal eigenvalues, has often been interpreted as a physical oscillation. But if the time series contains red noise, such pairs of eigenvalues and T-EOFs can occur even though physical oscillations may not be present in the time series. Therefore, Allen and Smith (1994) proposed a Monte Carlo technique to estimate the probability of pairs of approximately equal eigenvalues representing distinct physical oscillations. Briefly, a red noise model is assumed and its parameters are estimated from the time series. A large number of realizations of the red noise process are generated and a lag-covariance matrix is estimated from each simulated time series. These matrices are projected onto the T-EOFs of the original time series to estimate eigenvalues. If the kth eigenvalue from the SSA of the original time series lies above some specified limit of the corresponding distribution of kth eigenvalues of the simulated time series, the kth T-EOF would not be attributable to the assumed red noise process. In the present analysis, the autoregressive model of order one [AR(1)] was assumed as the red noise process. Lag-one autocorrelation and variance of each time series to be analyzed were estimated, and 10 000 time series having the same length as the original time series were simulated using these parameters in the AR(1) model. The Broomhead and King (1986) algorithm was used to estimate lag-covariance matrices. Confidence limits on the eigenvalues of the lag-covariance matrix of the original time series were estimated from the 10 000-member distribution for each eigenvector.

The maximum entropy method (MEM; see, e.g., Burg 1978; Ulrych and Bishop 1975) of spectrum analysis was also used. Press et al. (1987) have described the theoretical and computational aspects of this technique. Penland et al. (1991) adapted the MEM to achieve high spectral resolution without contamination due to spurious spectral peaks by applying an SSA filter to the time series under study to remove much of the uncorrelated noise in the time series and then applying the MEM to the SSA-filtered time series. This combined spectral analysis technique is referred to as the SSA-MEM in the following sections.

To analyze decadal variations as a function of time, the wavelet transform (Meyers et al. 1993; Gu and Philander 1995; Lau and Weng 1995) and moving-window Fourier transform (MWFT) were estimated for several window widths. The Morlet wavelet (see, e.g., Gu and Philander 1995) was used as the basis function for the wavelet transform.

b. Analysis of spatial structures

Real and complex EOF analyses were used to isolate large-scale and dominant space-time structures of SST variations. Several versions (see MD for details) of real EOF analyses were used. Horel (1981, 1984) and Barnett (1983) have described rotated and complex EOF techniques. In the complex EOF (CEOF) technique applied in the present study, the Hilbert transform of SST anomalies was estimated using the Fourier method (Barnett 1983). Distinctness of eigenvalues and the consequent independence of the corresponding real or complex eigenvectors was estimated with the formula developed by North et al. (1982) based on sampling errors in the data.

5. Spatiotemporal structures of the tropical Atlantic SST variations

As described in section 3, annual-average SST anomaly time series over the Atlantic Ocean were extracted from the GOSTA. Linear trends of SST anomaly series versus time were computed and removed from the time series in each grid box before further analyses of the time series. The linear trend everywhere in the tropical Atlantic was toward warmer SSTs during the 110-yr analysis period. The tropical North Atlantic SSTs warmed 0.3°–0.4°C and the tropical South Atlantic SSTs warmed 0.5°–0.6°C during the analysis period. A detailed analysis of these trends and their causes is beyond the scope of the present study. After removing linear trends, spatiotemporal structures of decadal timescale SST variations were analyzed. They are described and discussed in this section.

a. The dipole SST pattern, its physical interpretation, and decadal timescales

1) THE DIPOLE SST PATTERN

As mentioned earlier in section 2, much of the previous work on the tropical Atlantic SST variations used real EOF analysis to isolate dominant statistical patterns of SST variations. These EOF analyses had revealed a statistical pattern of SST variations having opposite signs in the tropical North and South Atlantic; this statistical dipole pattern was frequently assumed to be a dynamical–thermodynamical mode of tropical Atlantic SST variations. Regressions between rainfall anomalies over Nordeste Brazil and tropical Atlantic SST anomalies had also revealed a similar dipole pattern. To see if such a dipole pattern emerges from the 110-yr SST data analyzed in the present work and to develop, if possible, a physical interpretation of such a pattern, real EOFs of the 110-yr SST data were calculated.

EOF1 of the Atlantic SST anomalies between 30°S and 30°N, its corresponding principal component (PC) time series, the variance ''explained'' by PC1 time series in each grid box, and the Fourier and SSA – MEM spectra of PC1 time series are shown in Fig. 1. The first and second EOFs – PCs explain approximately 32% ± 4% and 15% ± 2%, respectively, of the total SST variance in the domain. The first and second EOFs – PCs are statistically independent according to North et al.'s (1982) formula based on the estimated sampling errors in the data. EOF1 pattern (Fig. 1a) contains two centers of activity; one in the tropical southeast Atlantic and the other in the tropical North Atlantic. The variance explained (Fig. 1b) by PC1 time series in each grid box also shows that approximately 40%–50% of the SST variance in these two regions is due to EOF1 – PC1. There is a small amount (10%–30% explained variance) of SST variations due to EOF1 – PC1 near the equator.

The estimated Fourier spectrum (Fig. 1d) of PC1 time series contains the highest peak at approximately 12–13 yr and the next highest peak at approximately 40 yr. The spectral density of the 12–13-yr peak exceeds the 95% limit obtained with the Monte Carlo technique described in section 4. Chance occurences of spectral peaks were also tested with the Monte Carlo technique and it was found that there is 90%–95% probability that the 12–13-yr peak did not occur due to chance.

As mentioned in section 4, a combination of the SSA and MEM techniques was also used to estimate the spectrum of PC1 time series. To reduce the order of the AR model used in the MEM and thus reduce the occurrence of spurious spectral peaks in the MEM spectra, the SSA-filtered version of PC1 time series was used. The first 10 SSA components, containing 60% of the total PC1 variance, were recombined. PC1 time series and its SSA-filtered version (Fig. 1c) show SST variations at various timescales during the 110-yr period from 1882 to 1991, prominent among them are the decadal–multidecadal timescales. The AR models of various orders were fitted to the SSA-filtered PC1 time series and the optimum model order was selected using Akaike's information criterion (Press et al. 1987). The MEM spectrum of the SSA-filtered PC1 time series was then calculated using the optimum AR model. This SSA – MEM spectrum is shown in Fig. 1d. This spectrum also contains the highest peak at approximately 12–13 yr and the next highest peak at approximately 40 yr as does the FSA spectrum. Thus, the dominant EOF – PC of the tropical Atlantic SST anomalies is a cross-equatorial, dipole pattern that oscillates, among other periods, at approximately 12–13-yr period. Since the SST time series are only 110 yr long, the 40-yr spectral peak should be considered only suggestive.

EOF2 pattern (not shown) contains variations of the opposite signs between the tropical Atlantic and the subtropical South Atlantic. There is an indication of larger amplitudes near the eastern boundaries of the tropical North and South Atlantic Oceans. The associated PC2 time series shows variations at various timescales but its spectrum contains many peaks, among them the decadal–multidecadal peaks, and is generally ''red.''

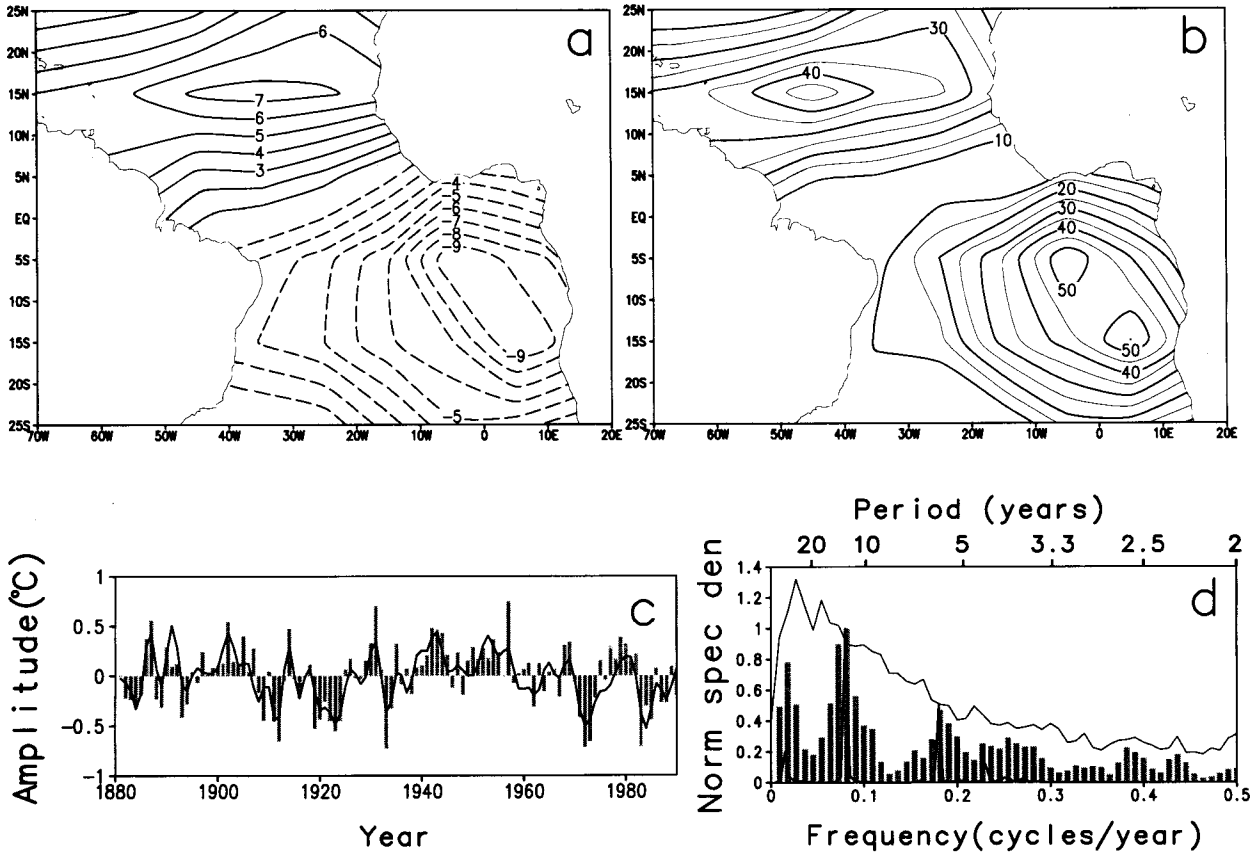

FIG. 1. Empirical orthogonal function (EOF) analysis over 30°S–30°N. Annual-average SST anomalies from the *GOSTA* were used. (a) First EOF multiplied by 10 (contour interval one unit), (b) percent of the total variance explained by the first principal component (PC) in each grid box (thick contour interval 10%, interval between thick and thin contours 5%), (c) PC1 (°C) time series (bars) and SSA-filtered (line) PC1 time series, and (d) estimated normalized Fourier spectral density (bars) of PC1 time series, the 95% confidenece level (light line) for the Fourier spectral peaks obtained with the Monte Carlo technique, and the normalized SSA – MEM spectral density (heavy line) of PC1 time series. EOF1 – PC1 explain 32% ± 4% of the total SST variance in the domain.

Therefore, EOF2 – PC2 may contain contributions from several phenomena.

To analyze only the low-frequency SST variance, EOFs–PCs of filtered SST anomalies were computed. The low-pass Fourier filter allowed only periods greater than or equal to 8 yr to pass through without any attenuation of amplitude and completely eliminated all periods shorter than 8 yr. The first two EOF patterns of the filtered SST anomalies are similar to those in which filtering was not used. The corresponding PC time series show decadal–multidecadal variations similar to those in the unfiltered case.

These results of the EOF analysis of the 110-yr-long annual-average SST anomalies in 10° lat × 10° long grid boxes were also verified by using monthly average SST anomalies in 5° lat × 5° long grid boxes in the years 1952–91. During this period, continuous time series of monthly anomalies are available in the MOHSST5 dataset. The first two EOF patterns of the higher-resolution anomalies are substantially similar to the first two patterns of the annual-average anomalies. Decadal variations in the 40-yr-long, monthly average PC time series are also substantially similar to the decadal variations in the 110-yr-long, annual-average PC time series. Thus, the results of the various EOF analyses are consistent among themselves.

2) PHYSICAL INTERPRETATION OF THE DIPOLE SST PATTERN AND IDENTIFICATION OF DECADAL TIMESCALES

To develop a physical interpretation of EOF1 – PC1, spectral characteristics of SST anomaly time series near the two centers of activity (15°S–5°E and 15°N–35°W) and PC1 time series were compared. These three time series and their Fourier spectra are shown in Fig. 2. The correlation coefficient between the northern and southern time series is only −0.21, implying that SST variations in the tropical North and South Atlantic are not highly coherent. PC1 time series (Fig. 1c) has reasonably high correlation coefficients with the northern and southern time series (0.69 and −0.74, respectively), implying that there was some contribution from SST variations near both centers of activity to EOF1 – PC1 if

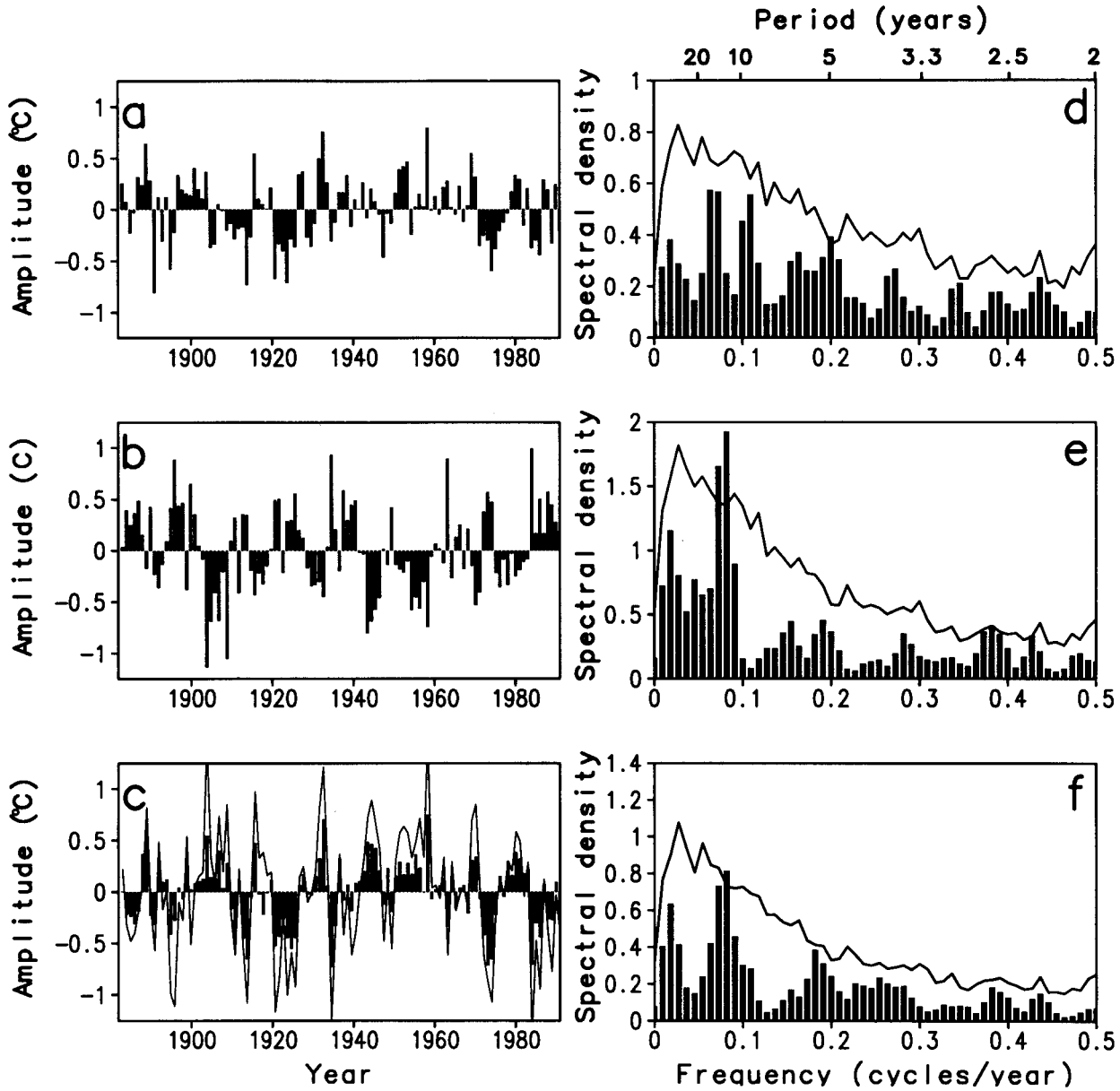

FIG. 2. (a) SST anomalies at 15°N–35°W, (b) SST anomalies at 15°S–5°E, and (c) SST PC1 (bars) and the difference (line) between SST anomalies in (a) and (b). The estimated Fourier spectral density of SST anomalies at (d) 15°N–35°W and (e) 15°S–5°E. (f) The estimated Fourier spectral density of SST PC1 time series. The lines in (d), (e), and (f) show the 95% confidence level obtained with the Monte Carlo technique.

all possible timescales were included in the calculation of correlation coefficients.

Following the suggestion by MD, based on analyses of tropical Atlantic SST anomalies simulated by the GFDL coupled ocean–atmosphere model, that the dipole EOF pattern may be interpreted as variations in the approximately north–south gradient of SST anomalies, the difference between the GOSTA SST anomalies at the northern and southern centers of activity in Fig. 1a were calculated. This difference is a measure of the approximately north–south gradient of SST anomalies and its time series is shown in Fig. 2c along with PC1 time series. A visual comparison of the two time series in Fig. 2c shows that the north–south gradient of SST anomalies (as measured by the difference in SST anomalies at the northern and southern centers) covaries with PC1 anomalies. The correlation coefficient between the two time series is 0.92. Therefore, it appears that EOF1 – PC1 should be interpreted as variations of the cross-equatorial gradient of SST anomalies.

The estimated Fourier spectra of the northern and southern SST anomaly time series, and PC1 time series

are shown in Figs. 2d–f. The decadal peak is most prominent and significant at 95% level in the spectrum of the southern time series (Fig. 2e); it is also present and barely significant in the spectrum of PC1 time series (Fig. 2f). The spectrum of the northern time series (Fig. 2d) appears red. There are decadal peaks in it but they are much below 95% significance level and their spectral densities are approximately a factor of 3 smaller than the spectral density of the southern decadal peak. Fourier cross-spectrum analysis of the northern and southern time series showed that the squared coherence between the two at the 12–13-yr period is 0.5 and not significant at 95% level. At the 8–9-yr period, where there is a peak in the northern spectrum but not in the southern spectrum, the squared coherence is 0.65. These coherences may not have any physical significance because of the absence of significant peaks in both spectra at these two periods. Therefore, the Fourier spectrum and cross-spectrum analysis confirm that decadal SST variations in tropical Atlantic SSTs are not because of a coherent, cross-equatorial dipole mode of variability.

Results of other analyses also point toward similar conclusions. The SST anomaly time series at 15°N–35°W and 15°S–5°E, and the PC1 time series were analyzed with the SSA technique. Physical significance of SSA eigenvalues was estimated with the Monte Carlo technique described in section 4. Eigenvalues of lag-covariance matrices of the three time series are shown in Figs. 3a–c with 99%, 95%, and 90% Monte Carlo confidence limits. Results for 40-lag window widths are shown. Eigenvalue spectrum (Fig. 3a) of the tropical North Atlantic SST anomaly time series shows the presence of pairs of eigenvalues, significant at 95%, for T-EOFs 3–4 and 5–6. Eigenvalue spectra (Figs. 3b and 3c) of the tropical South Atlantic SST anomaly and PC1 time series show the presence of pairs of eigenvalues, significant at 99%, for T-EOFs 1–2. Eigenvalues for T-EOFs 3–4 for PC1 time series are also significant at 90%. Reconstructed time series corresponding to these three significant pairs of T-EOFs and T-PCs (3–4 for the tropical North Atlantic, 1–2 for the tropical South Atlantic, and 1–2 for PC1 time series) are shown in Figs. 3d–f along with each original time series. The three pairs of eigenvalues explain approximately 12%, 31%, and 24% of the total variance of each of the three time series, respectively. The reconstructed time series (Fig. 3d) for the tropical North Atlantic shows oscillations at 5–6-yr average period. The six T-EOFs and T-PCs for the tropical North Atlantic that are significant above 90% do not have decadal oscillations. The reconstructed time series (Figs. 3e–f) for the tropical South Atlantic and PC1, however, have relatively high-variance decadal oscillations at 12–13-yr average period, which is also the dominant (and significant) period in the Fourier spectra (Figs. 2e–f) of these two time series. This difference in the spectra, Fourier and singular, of tropical North and South Atlantic SST anomaly time series was also apparent in MD's results. Decadal oscillations in the reconstructed time series (Figs. 3e–f) match the apparent decadal variations in the original time series (bars in Figs. 3e–f) reasonably well. Figures 3e and 3f also show that there is a very high correlation between the decadal oscillations in the tropical South Atlantic SST and PC1 time series. When the negative sign of EOF1 pattern in Fig. 1a in the tropical South Atlantic is included in the comparison, the correlation coefficient between the two decadal oscillations time series (Figs. 3e–f) is 0.88, implying that approximately 80% of the coherent decadal variance in the cross-equatorial dipole EOF1 pattern is explained by coherent decadal oscillations in the tropical South Atlantic SSTs. The reconstructed time series of decadal oscillations in the tropical South Atlantic SSTs (Fig. 3e) also shows that its amplitude has decreased since the 1950s. As shown in section 6a, these decadal oscillations in the tropical South Atlantic SST and PC1 agree reasonably well with variations in the north Nordeste Brazil rainfall.

The wavelet analysis of the SST anomaly time series at 15°N–35°W and 15°S–5°E, and PC1 time series confirm the results of the SSA analysis. The real modulus of the wavelet transform of these three time series is shown in Fig. 4. The ''cone of influence'' (Gu and Philander 1995) at decadal timescales restricts the most reliable results to early 1910s–early 1960s in the present analysis. During this period, there were negligible decadal variations in the tropical North Atlantic SSTs (Fig. 4a), whereas the amplitude of decadal variations in the tropical South Atlantic SSTs (Fig. 4b) was approximately three to four times larger during the same period and some of the largest decadal variations in PC1 time series also occurred during this period. Outside the cone of influence there are two periods (1890s–1910s and 1960s–early 1980s) during which the SSTs at both the tropical Atlantic locations underwent decadal variations. During both periods, the amplitude at the tropical South Atlantic location was much larger than the amplitude at the tropical North Atlantic location. MWFT spectrum analyses (not shown) of these three time series confirm the SSA and wavelet analyses results.

Thus, the real EOF and various spectrum analyses of tropical Atlantic SST anomalies show that the dipole EOF pattern and the associated PC time series should be interpreted as variations in the approximately north–south, cross-equatorial SST gradient and not as a dipole mode of cross-equatorial SST oscillations (see the discussion about statistical patterns and physical modes in section 2). Moreover, these analyses also show that coherent decadal oscillations in the cross-equatorial SST gradient are largely due to coherent decadal oscillations in the tropical South Atlantic SSTs and that there is a distinct decadal (12–13 yr) oscillation timescale in tropical South Atlantic SSTs but not in tropical North Atlantic SSTs.

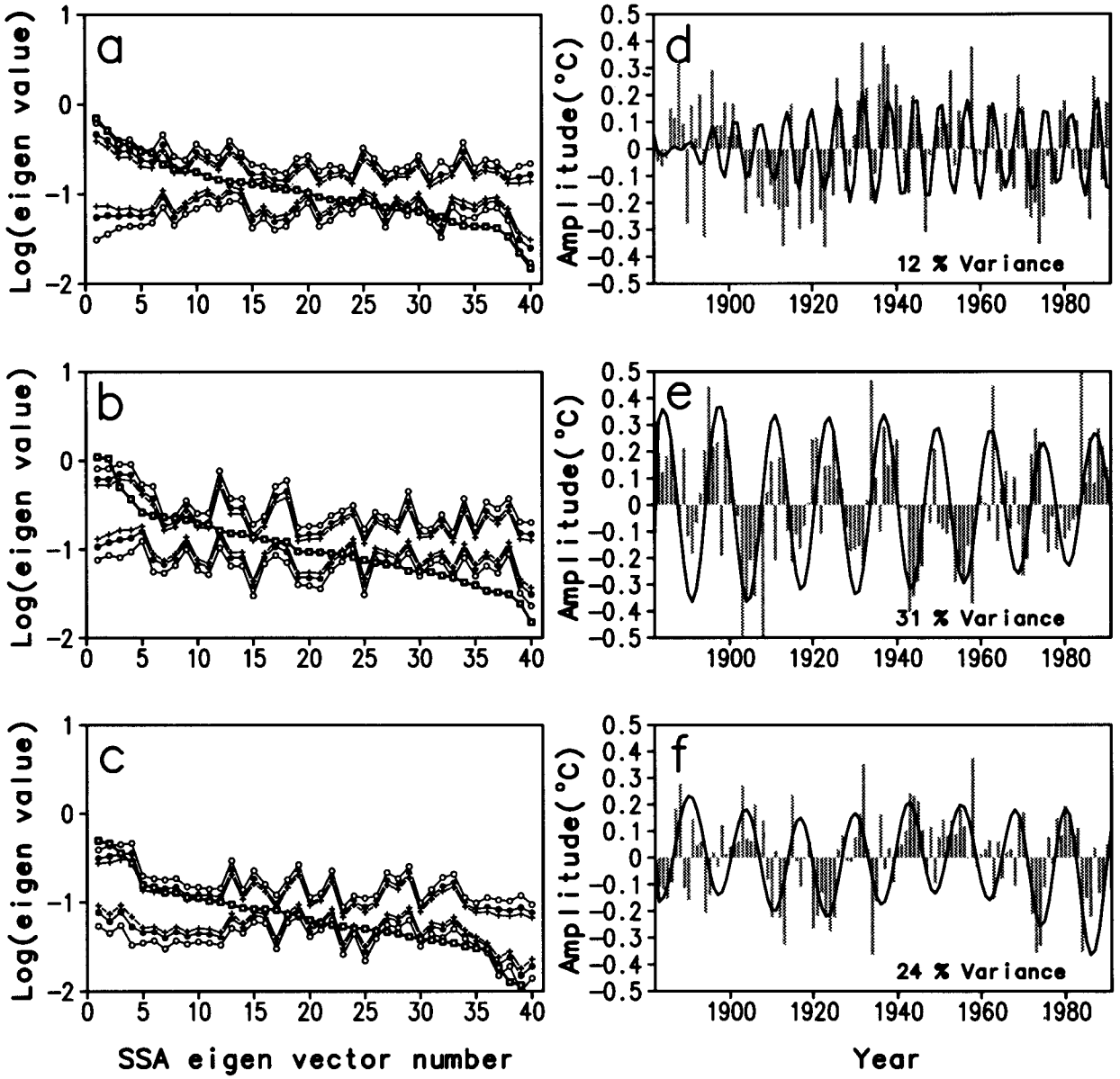

FIG. 3. SSA eigenvalue spectra (box), and the 99%–1% (open circle), 95%–5% (dot), and 90%–10% (cross) Monte Carlo confidence limits for SST anomaly time series (a) 15°N–35°W, (b) 15°S–5°E, and (c) PC1. (d), (e), and (f) Original SST anomaly time series (bar) and reconstructed SSA components (line) corresponding to (a), (b), and (c), respectively. The amount of variance in reconstructed SSA components is given in (d), (e), and (f).

b. Evolution of decadal SST anomalies and Tropics–extratropics interaction

As the earlier-described analyses showed, decadal SST gradient variations were apparently caused by largely independent SST variations on two sides of the equator during the analysis period. Further clarifications of the cross-equatorial SST gradient variations and SST variations on two sides of the equator were obtained by analyzing the evolution of decadal SST anomalies on two sides of the equator independently. The evolution of Atlantic decadal SST anomalies was analyzed with the CEOF technique and also by plotting sequences of maps of decadal bandpass-filtered SST anomalies. The CEOF technique was used to isolate energetic empirical patterns of SST variations in which phase differences among grid boxes may be other than 0° or 180°, and to allow each empirical pattern to contain stationary and traveling SST variations if such variations were present in the SST anomaly data. Separate CEOF calculations for the North and South Atlantic also ensured that CEOF patterns were not forced by the choice of the domain to have interhemispheric connections that may not be

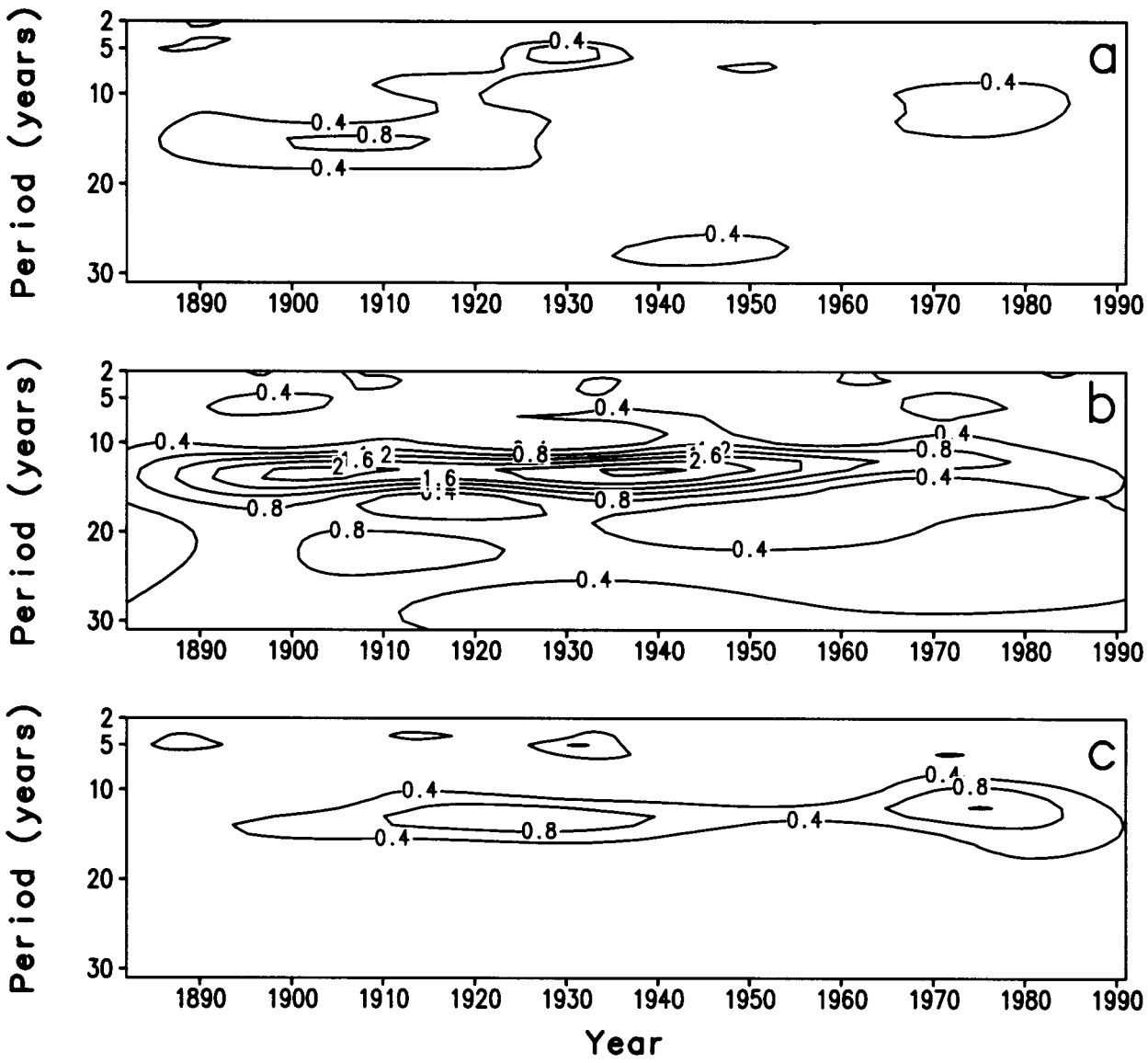

FIG. 4. Real modulus of the wavelet transform of SST anomaly time series at (a) 15°N–35°W and (b) 15°S–5°E. (c) Real modulus of the wavelet transform of PC1 time series.

physical. The analysis domain was expanded from the tropical Atlantic to 40°S and 60°N in order to see if Tropics–extratropics interaction played a role in the evolution of decadal SST anomalies in the tropical Atlantic during the analysis period.

1) COMPLEX EMPIRICAL ORTHOGONAL FUNCTION ANALYSIS

CEOFs and complex principal components (CPCs) were calculated for various geographical domains, and without and with applying a low-pass filter to the SST anomaly data. When applied, the low-pass Fourier filter allowed all oscillation periods equal to or greater than 8 yr to pass through without any attenuation in their amplitudes and completely attenuated amplitudes of all other oscillations. The CEOFs shown here are plotted so that the length of each vector is proportional to the magnitude of the spatial amplitude function in each grid box and the direction of the vector indicates relative spatial phase. A vector pointing from west to east is used as the reference phase. Motion of anomalies is implied in the direction (latitude or longitude) in which vectors rotate counterclockwise. CPCs are decomposed into amplitude and phase time series, and these time series are plotted separately. Derivatives of phase with respect to time can be interpreted as frequencies of SST variations.

The dominant and relevant (for the tropical Atlantic) CEOFs – CPCs of low-pass-filtered SST anomalies in

each hemisphere are shown and described here. CEOFs 1, 2, 3, and 4 of low-pass-filtered North Atlantic SST anomalies (referred to as NCEOFs hereafter) explain 47% ± 6%, 17% ± 2%, 12% ± 2%, and 7.1% ± 1% variance, respectively. These four NCEOFs are independent of one another and of subsequent NCEOFs. NCEOF1 contains (not shown) SST variations in approximately the same phase over the entire North Atlantic. Much of the variation in the amplitude and phase of NCPC1 (not shown) is contained in a multidecadal oscillation from the mid-1910s to mid-1970s with approximately 0.5°C amplitude. Variations before and after this multidecadal oscillation episode do not appear to occur at any distinct timescale. NCEOF2 (not shown) contains spatially stationary SST variations at opposite phases between the northwestern Atlantic regions north and south of Newfoundland. Thus, NCEOF1 – NCPC1 and NCEOF2 – NCPC2 contain largely spatially stationary variations that are either not at decadal timescales or are not in the tropical Atlantic. They bear some resemblence to the real EOF1 – PC1 and EOF2 – PC2 of winter SST anomalies calculated by Deser and Blackmon (1993).

NCEOF3 and NCEOF4 have significant amplitudes in the tropical Atlantic, and undergo decadal variations. In NCEOF3 (Fig. 5a), the spatial phase variation north of 40°N implies strong west to east motion of SST anomalies from the North American coast to the European coast, strong southward motion along the European–African coasts from mid- to high latitudes into tropical latitudes, and then moderate-to-weak motion from the African coast to the western Atlantic–Caribbean. SST variations in the mid- to high latitudes and tropical latitudes are at approximately opposite phases. The amplitude and period of SST variations in NCPC3 (Figs. 5b,c) show large variations and do not show a distinct decadal timescale. In NCEOF4 (Fig. 6a), a counterclockwise rotation of vectors at 35°N from the eastern to the western Atlantic implies motion of SST anomalies from the eastern to the western Atlantic. In the western Atlantic, an opposite-phase oscillation in SST anomalies near Newfoundland and the tropical–subtropical Atlantic is apparent. Eastward motion of SST anomalies is implied at 45°N. Starting from the African coast, SST anomalies move southward in the tropical northeastern Atlantic. The amplitude and phase of NCPC4 (Figs. 6b,c) show variations but do not show a distinct decadal timescale. Thus, the major characteristics of NCEOF3 are nearly opposite phases of SST variation between the tropical and mid-high latitude North Atlantic and clockwise rotations of SST anomalies starting from the northeast coast of North America and ending in the tropical western Atlantic–Caribbean. SST anomalies in NCEOF4 appear to originate mainly near the African coast, and spread westward across the North Atlantic and southward toward the equator. Weak eastward motion is also apparent at 15°N in NCEOF4. The variances explained by NCEOF3 – NCPC3 and NCEOF4 – NCPC4 are significantly different, and their spatial and temporal scales are also different, therefore it is not likely that the CEOF technique has decomposed a stationary oscillation into two oscillations traveling in opposite directions. Thus, NCEOF3 – NCPC3 and NCEOF4 – NCPC4 appear to be physically independent patterns of decadal SST variations in the tropical-midlatitude North Atlantic. The absence of a distinct decadal timescale in NCPC3 and NCPC4 is consistent with Fourier, singular, and wavelet spectra of the tropical North Atlantic SST time series (Figs. 2d, 3d, and 4a) and with these three types of spectra of extratropical North Atlantic SST time series (not shown).

CEOFs 1, 2, and 3 of low-pass-filtered South Atlantic SST anomalies (referred to as SCEOFs hereafter) explain 38% ± 5%, 22% ± 3%, and 11% ± 2% variance, respectively. These three SCEOFs are independent of one another and of subsequent SCEOFs. Only SCEOF1 (Fig. 7a) has relatively large amplitudes in the tropical South Atlantic. The spatial phase variation in SCEOF1 implies propagation of anomalies from the African coast to the South American coast between the equator and 30°S. Anomalies also propagate down the South American coast from the equator to 40°S. SST variations in SCEOF1 have approximately 90°–120° phase differences between the equator–20°S lat band and the southwestern corner (30°–40°S) of the domain. The SCPC1 amplitude (Fig. 7b) is generally larger than the NCPC3 and NCPC4 amplitudes, and shows large, multidecadal variations. The SCPC1 phase variations (Fig. 7c) imply approximately 13-yr average period. Fourier, singular, and wavelet spectra of real EOF1-PC1 and SST anomaly time series at 15°S–5°E (Figs. 1, 2, and 3) also show the presence of the 13-yr period in the tropical South Atlantic SST variations.

The dominant CEOFs – CPCs for domains spanning 30°S–30°N and 40°S–60°N, and calculated without and with the low-pass filter confirmed the results of the independent CEOF analysis in each hemisphere. The dominant CEOFs – CPCs spanning both hemispheres did not have any distinct decadal timescale of SST variations, decadal SST variations in the tropical North and South Atlantic appeared to be largely independent, and suggested possible connections between tropical and extratropical SST variations in each hemisphere. Therefore, the application of the low-pass filter and the independent calculation of CEOFs in each hemisphere were appropriate.

2) Evolution of decadal SST anomalies

The CEOF analysis yielded statistical and perhaps physical characteristics of evolution of decadal variations in the tropical-midlatitude Atlantic SSTs. It is also very important to know if these statistical characteristics were representative of individual life cycles of decadal SST anomalies. Therefore, decadal SST anomalies were reconstructed from CEOFs – CPCs relevant for the tropical Atlantic. Life cycles of these reconstructed decadal

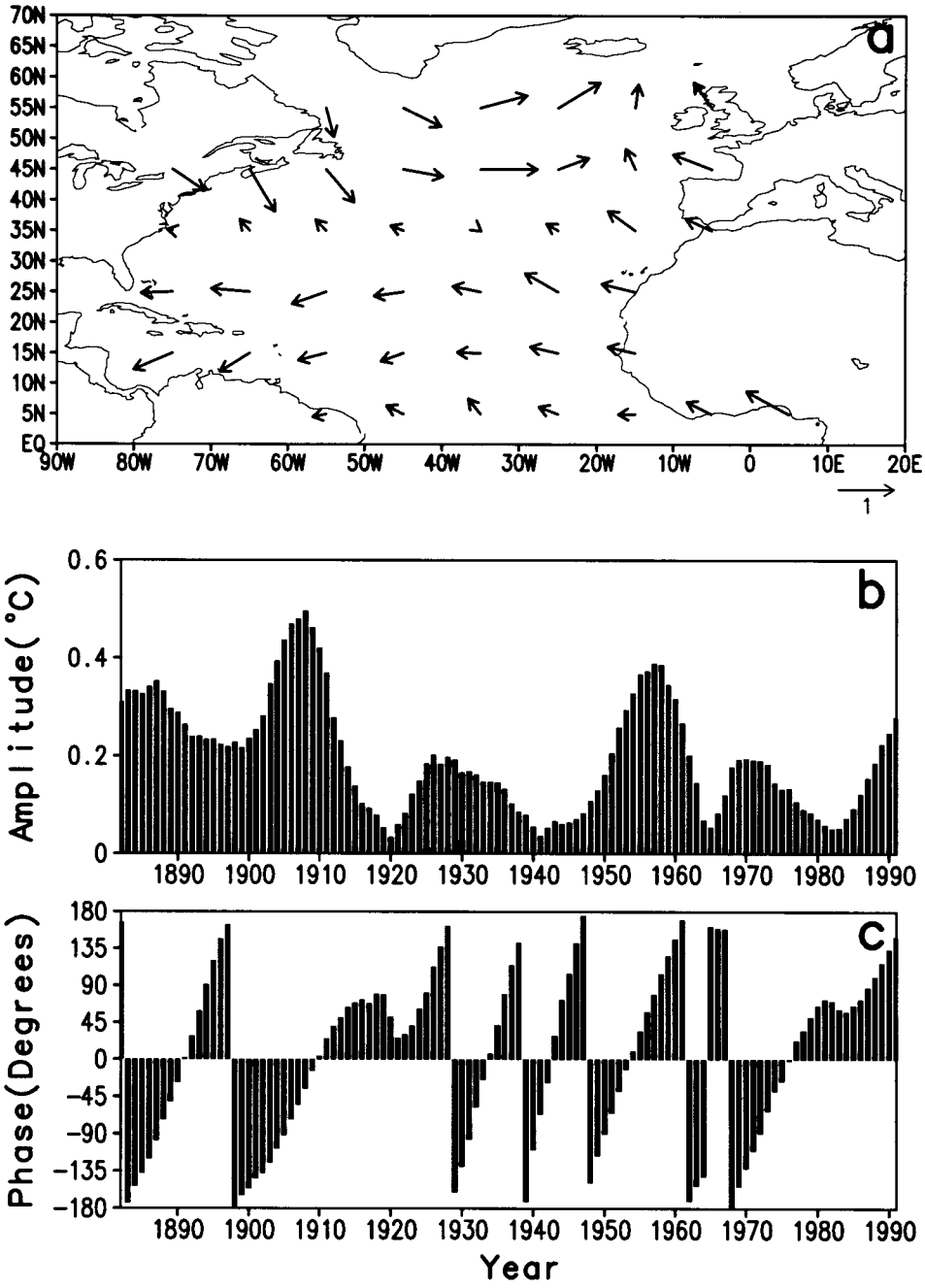

FIG. 5. (a) Complex EOF3 (NCEOF3) of the low-pass-filtered North Atlantic (0°–60°N) SST anomalies. The vector scale is shown near the lower-right corner of the box. (b) Amplitude (°C) and (c) phase of complex PC3 (NCPC3). NCEOF3 – NCPC3 explain 12% ± 2% of the total SST variance in the domain.

SST anomalies were then compared with life cycles of decadal bandpass-filtered SST anomalies. Generally, decadal SST anomalies obtained with these two techniques agreed reasonably well, but since two, possibly physical, decadal variations in the North Atlantic were identified from the results of the CEOF analysis, decadal SST anomalies reconstructed from these two NCEOFs – NCPCs are shown separately. Decadal SST anomalies in the North Atlantic were independently reconstructed from NCEOF3 – NCPC3 and NCEOF4 – NCPC4 for the entire 110-yr analysis period, but the anomalies for years 1949–60 (NCEOF3 – NCPC3) and 1972–83 (NCEOF4 – NCPC4) are shown because the respective NCPC amplitudes (Figs. 5b and 6b) were relatively large during these years. As described earlier, only SCEOF1 – SCPC1 has relatively large amplitudes in the tropical

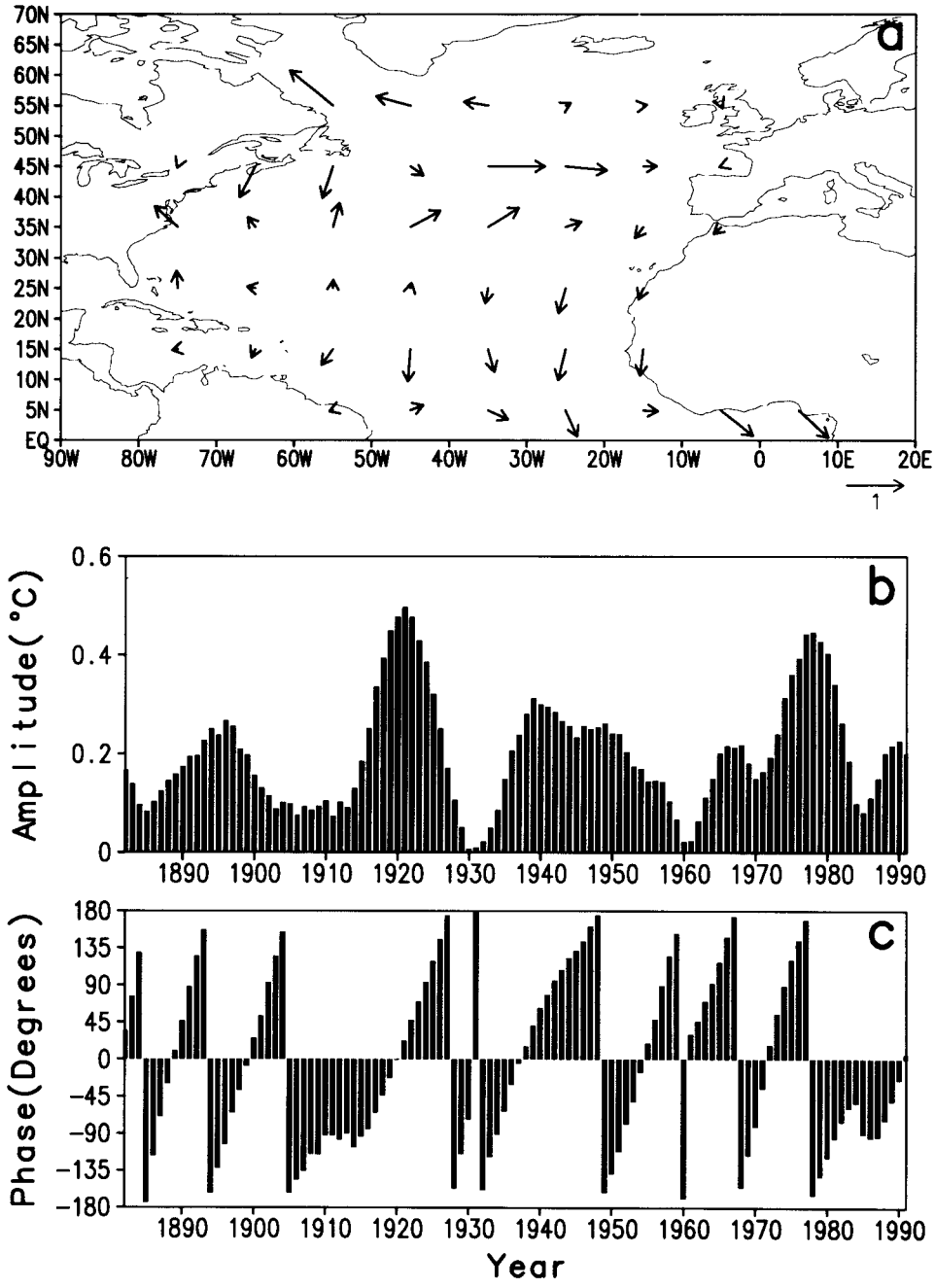

FIG. 6. As in Fig. 5, for NCEOF4 – NCPC4 explaining 7% ± 1% of the total SST variance in the domain.

South Atlantic, therefore the South Atlantic decadal SST anomalies were reconstructed from SCEOF1 – SCPC1 during the same years as the reconstructed North Atlantic anomalies.

During 1949–60 (Fig. 8), reconstructed positive or negative SST anomalies from NCEOF3 – NCPC3 moved eastward from the North American coast north of 35°N, reached the European–African coast, traveled southward and westward in the tropical North Atlantic, and then northward in the western Atlantic. Thus, the anomalies appeared to travel clockwise in a partial or complete circle in the North Atlantic. The maximum amplitude of these SST anomalies was 0.15°–0.2°C. From the tropical North Atlantic, these anomalies sometimes spread across the equator in the tropical South Atlantic, but amplitudes were generally smaller in the tropical South Atlantic during these years. The clockwise motion of these SST anomalies in the North At-

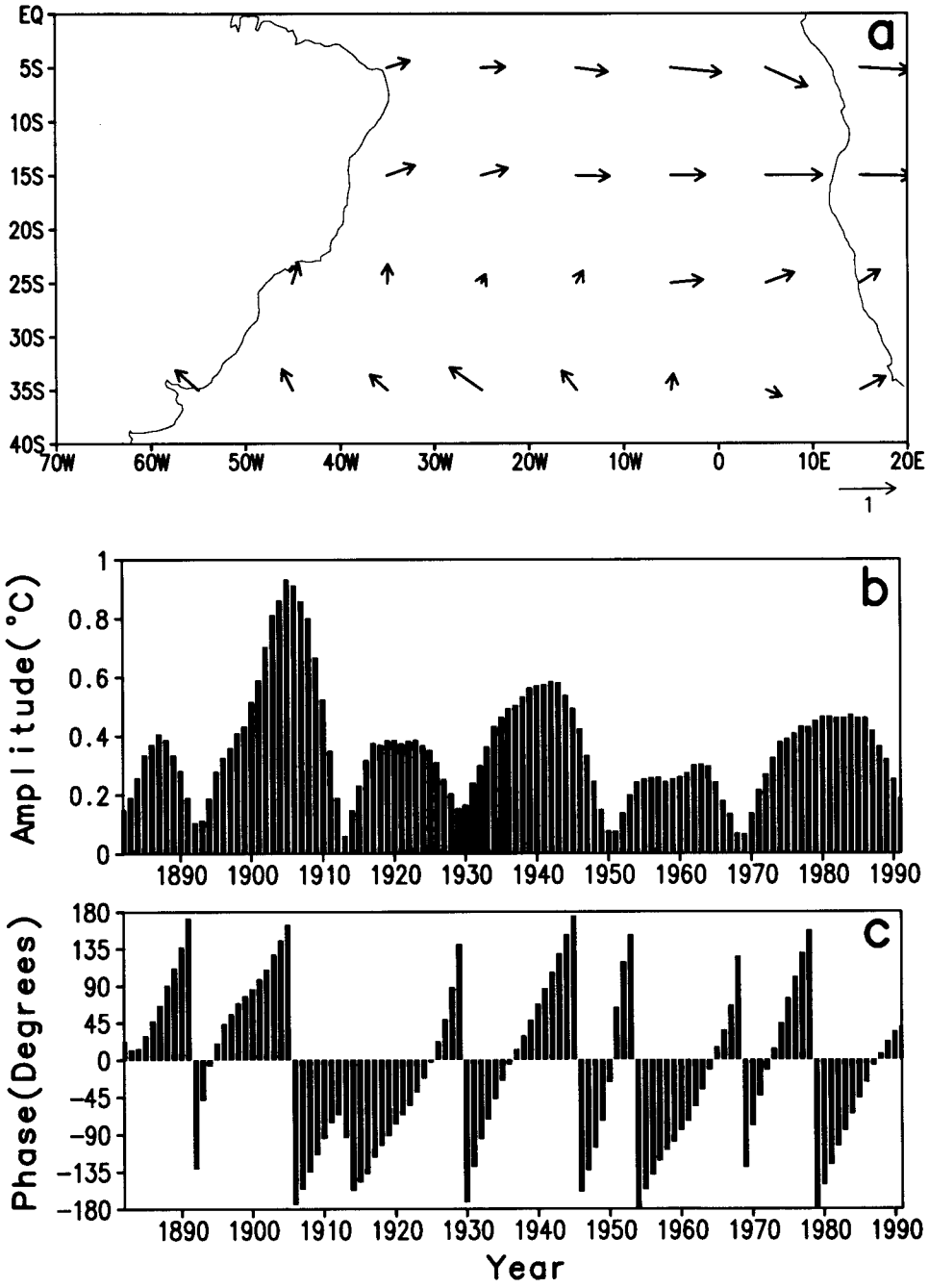

FIG. 7. (a) Complex EOF1 (SCEOF1) of the low-pass-filtered South Atlantic (0°–40°S) SST anomalies. The vector scale is shown near the lower-right corner of the box. (b) Amplitude (°C) and (c) phase of complex PC1 (SCPC1). SCEOF1 – SCPC1 explain 38% ± 5% of the total SST variance in the domain.

lantic created the appearance of north–south and east–west dipole patterns in the North Atlantic, but not of a cross-equatorial dipole pattern. Reconstructed NCEOF3 – NCPC3 anomalies evolved similarly during other epochs of relatively large NCPC3 amplitude. As can be seen in Figs. 5b, 7b, and 8, the SCPC1 amplitude was considerably smaller than the NCPC3 amplitude during 1949–60. SST anomalies either spread from the tropical North Atlantic across the equator or there was in situ development of anomalies in the tropical South Atlantic (see the discussion in the last paragraph). The cross-equatorial SST gradient was perturbed by these decadal anomalies during this epoch as can be seen in Fig. 1c.

The decadal SST anomalies reconstructed from NCEOF4 – NCPC4 during 1972–83 (Fig. 9) first appeared in the tropical North Atlantic near the African

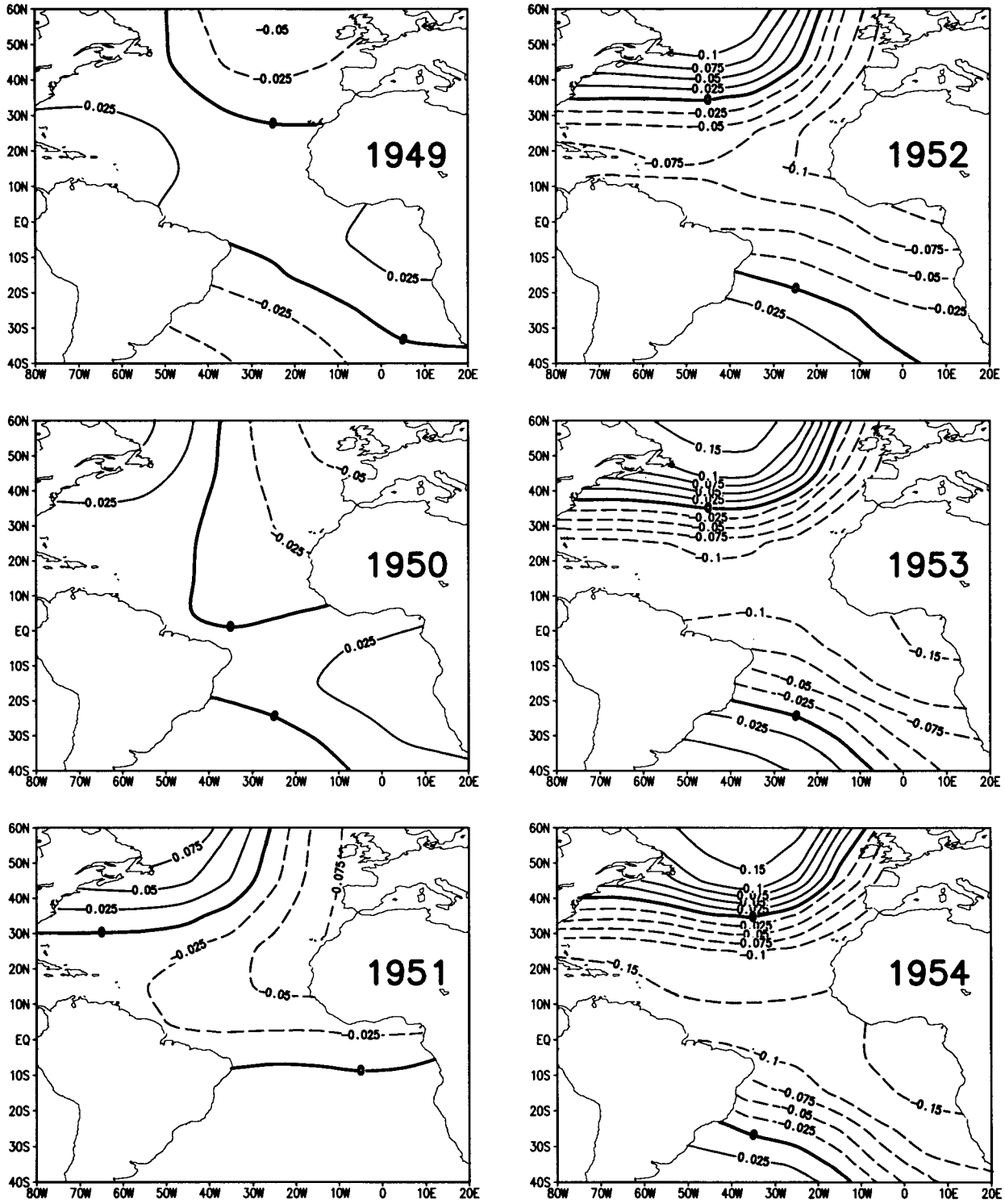

FIG. 8. SST anomalies (°C) reconstructed from NCEOF3 – NCPC3 and SCEOF1 – SCPC1 during 1949–60.

coast, and traveled northwestward and westward in the North Atlantic finally dissipating in the midlatitude central Atlantic. During these years, the decadal SST anomalies either spread southward from the tropical North Atlantic across the equator or there was in situ development of anomalies in the tropical South Atlantic (see the discussion in the last paragraph). The maximum amplitude of these decadal SST anomalies was 0.1°C

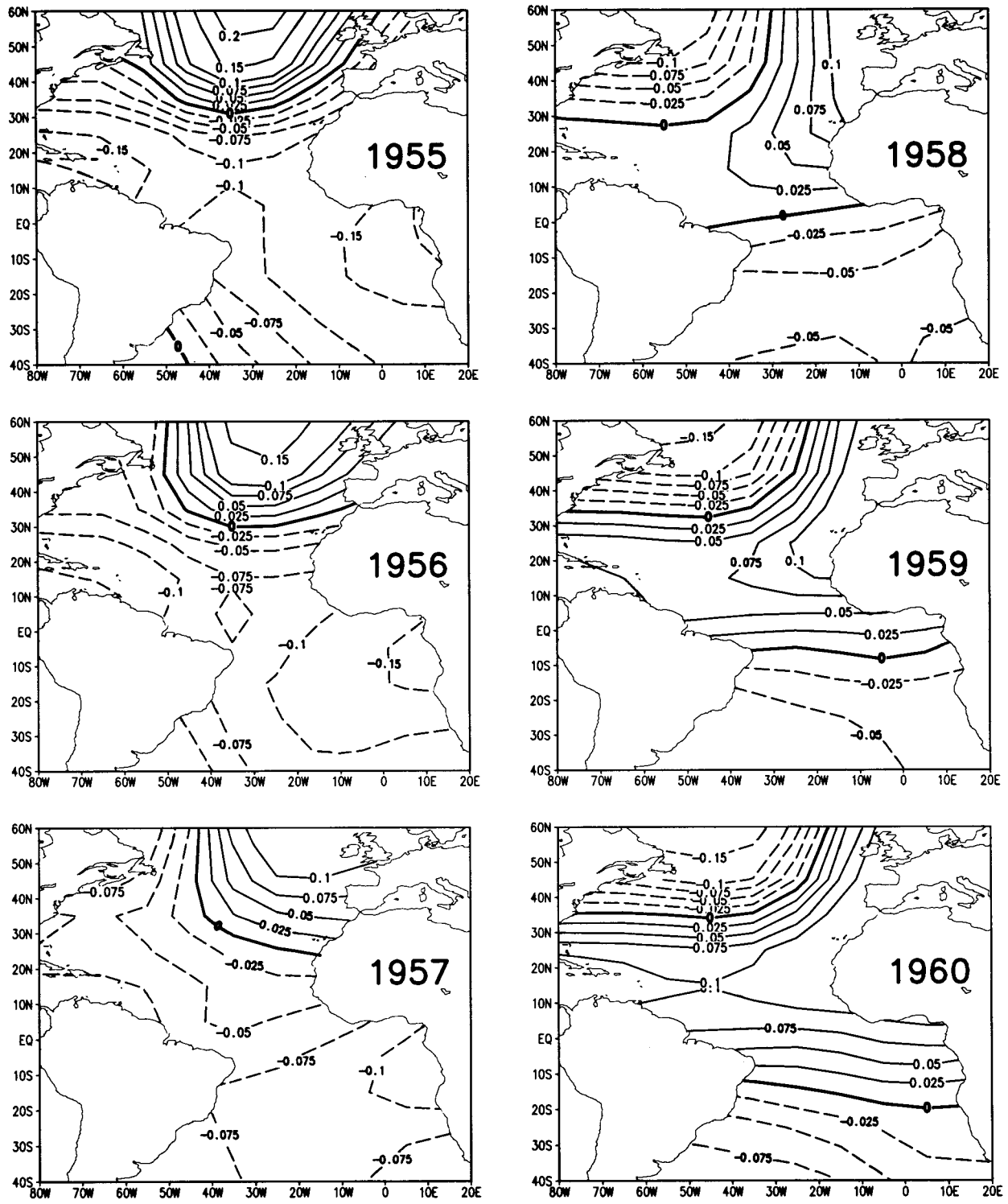

FIG. 8. (*Continued*)

in the North Atlantic and 0.25°C in the South Atlantic. This evolution of the SST anomalies occasionally created the fortuitous appearance of a cross-equatorial dipole but it is clear from Fig. 9 and from maps (not shown) of decadal bandpass-filtered SST anomalies that the anomalies on two sides of the equator evolved nearly independently and the amplitude in the tropical South Atlantic was much larger than the amplitude in the trop-

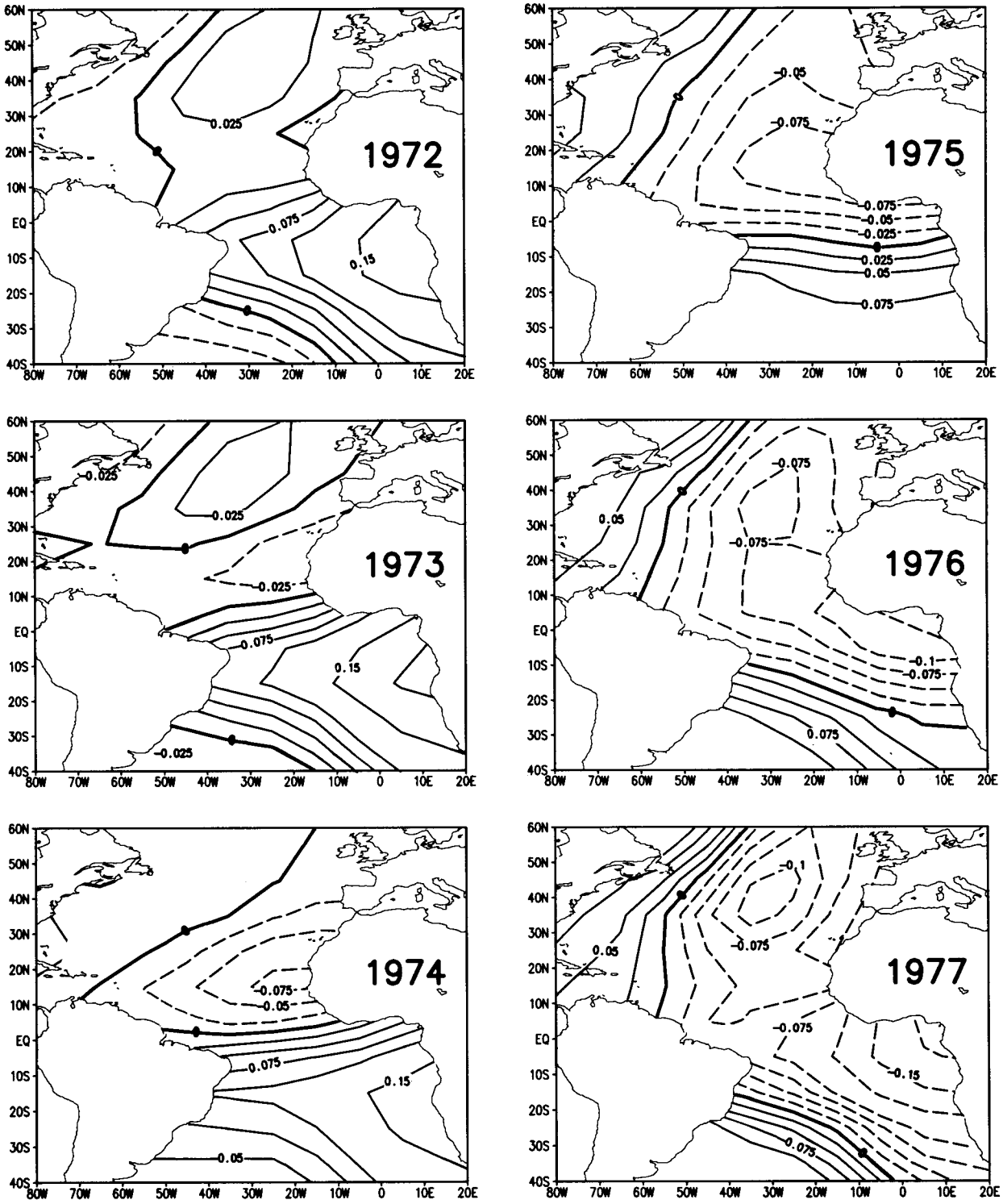

FIG. 9. SST anomalies (°C) reconstructed from NCEOF4 – NCPC4 and SCEOF1 – SCPC1 during 1972–83.

ical North Atlantic during 1972–83. NCEOF4 – NCPC4 and SCEOF1 – SCPC1 anomalies evolved similarly during other epochs of relatively large NCPC4 and SCPC1 amplitudes.

The analysis of evolution of decadal SST anomalies in the South Atlantic is hampered by the nonavailability of long SST anomaly time series in the mid-high latitude South Atlantic. But, in order to analyze evolution of the

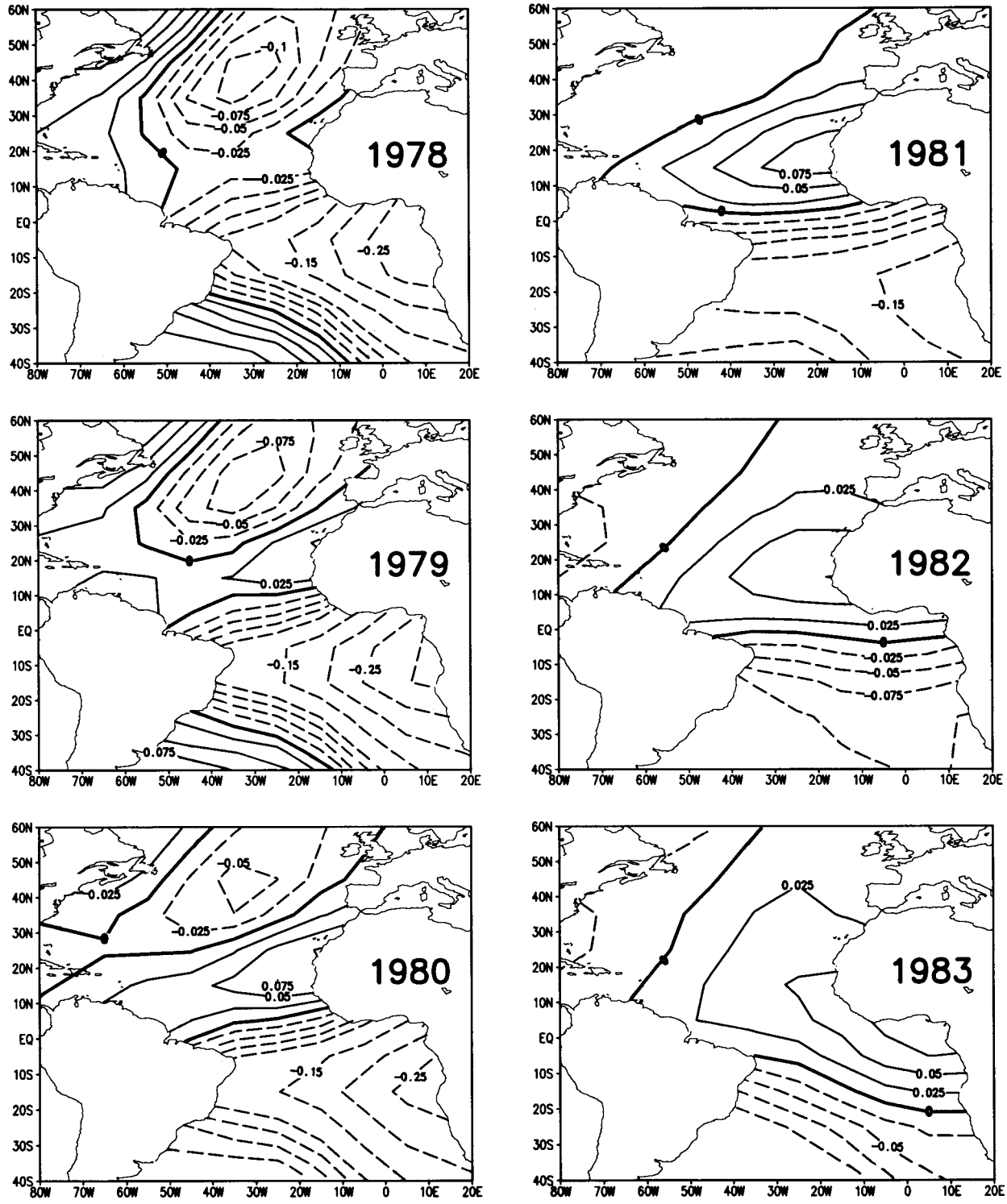

FIG. 9. (*Continued*)

South Atlantic SST anomalies in a different way, the 110-yr-long time series from 40°S to 60°N were filtered and maps of the filtered anomalies were plotted. The Fourier filter allowed amplitudes of 12–15-yr oscillations to pass through without any attenuation and completely attenuated amplitudes of all other oscillations. The 12–15-yr band was selected since Fourier, singular, and wavelet analyses (Figs. 2e, 3e, and 4b) of the trop-

ical South Atlantic SST anomaly time series showed the presence of the 12–13-yr distinct oscillation period. During epochs of relatively large amplitudes of these oscillations, sequences of maps (not shown) of the decadal bandpass-filtered SST anomalies suggest counterclockwise and occasionally clockwise rotations of anomalies around the tropical–subtropical South Atlantic. Evolution of SST anomalies reconstructed using the first four SCEOFs – SCPCs also suggest such rotations. In the North Atlantic, such rotations are contained in NCEOF3 – NCPC3, but in the South Atlantic such rotations are apparently distributed among several SCEOFs – SCPCs. These counterclockwise and clockwise rotations of decadal SST anomalies, however, appear to occur infrequently in both hemispheres.

c. Synthesis

The clockwise and counterclockwise rotations/variations of decadal SST anomalies in the North and South Atlantic, revealed by the CEOF analysis and maps of bandpass-filtered SST anomalies, appeared to be physical modes of variability of the Atlantic climate system during the 110-yr analysis period, although they appeared to occur at a distinct decadal timescale only in the tropical South Atlantic. Since the decadal SST variations were largest in the tropical Atlantic and the anomalies resided there for several years during each rotation/variation, the dominant real EOF of tropical Atlantic SST anomalies contained only a part of the rotations/variations as a cross-equatorial dipole. The less strong traveling anomalies along the eastern and western boundaries of the tropical Atlantic were mixed in the second EOF – PC, preventing a joint explanation of the first two EOFs – PCs as rotations/variations at decadal timescales. The SSA of PC1 time series (Fig. 1c) and of the SST anomaly time series at the two centers of action in real EOF1 (Fig. 1a) at 15°N–35°W and 15°S–5°E showed that there are decadal (12–13 yr) oscillations, represented as pairs of SSA eigenmodes, in PC1 and the tropical South Atlantic SST anomaly time series but not in the tropical North Atlantic SST anomaly time series. A high correlation (0.88) between the decadal oscillations in PC1 and the tropical South Atlantic time series implied that decadal oscillations in the cross-equatorial SST gradient time series are largely because of decadal oscillations in the tropical South Atlantic SSTs. This was confirmed by wavelet transform and MWFT analyses. The comparison among the SST anomaly time series at the two centers of action, the arithmatic difference between the two time series, and PC1 time series showed that the empirical dipole pattern should be interpreted as the cross-equatorial gradient of SST anomalies and not as a mode of oscillation of the tropical Atlantic climate system. The decadal SST gradient variations occurred due to nearly independent SST variations on two sides of the equator.

Thus, various analyses of the Atlantic SST anomalies revealed several aspects of decadal variations in the tropical Atlantic SST anomalies, including the evolution and physical interpretation of patterns of tropical Atlantic decadal SST variations. Only an EOF analysis of the tropical Atlantic grid box covariances would have resulted in misleading conclusions as has happened in the history of research in the tropical Atlantic SST variability.

6. Relationship between decadal variations in SST and other tropical Atlantic climate quantities

a. The north Nordeste Brazil rainfall

As mentioned in section 3b, normalized rainfall anomalies over north Nordeste Brazil from 1912 to 1985 were used in the present analysis. The time series of the rainfall anomalies (Fig. 10a) shows that there were variations at decadal-multidecadal timescales during the analysis period. The estimated Fourier spectrum (Fig. 10b) of the rainfall anomaly time series has peaks at approximately 12–13-yr, 5–6-yr, and 3–4-yr periods. The spectral densities at these periods exceed the 95% confidence level established with the Monte Carlo technique (see section 4). The estimated Fourier spectrum also has much smaller peaks at approximately 40–50-yr and 2.5-yr periods. As mentioned in section 2, numerous previous analyses (see the review in Hastenrath 1991) indicated that one of the distinct oscillation periods of the north Nordeste rainfall was approximately 14 yr. The present analysis confirms this earlier indication. In contradiction to the ''somewhat over two years'' (Hastenrath 1991) distinct oscillation period found in the previous analyses, however, the present analysis revealed distinct oscillation periods at 3–4 yr and 5–6 yr. Further discussion of these multiyear rainfall variations and its association with the tropical Atlantic SST variability is beyond the scope of the present study.

The north Nordeste Brazil rainfall time series was also analyzed with the SSA technique. Its SSA eigenvalue spectrum, along with Monte Carlo confidence limits, is shown in Fig. 10d. The first two eigenvalues, a pair, are almost significant at 99% limit and the next two at 90% limit. The first four eigenvalues explain 30% variance, and the corresponding T-EOFs and T-PCs show decadal–multidecadal variations. The reconstructed rainfall time series corresponding to these four eigenmodes is shown in Fig. 10c. For comparison, the reconstructed SST PC1 time series (Fig. 3f) is also shown in Fig. 10c. Decadal oscillations in the reconstructed rainfall time series agree reasonably well and are physically consistent with decadal oscillations in SST PC1. When the SST anomaly gradient in the tropical Atlantic was southward (northward), the north Nordeste Brazil rainfall was above (below) normal.

Fourier cross-spectrum analyses between the north Nordeste Brazil rainfall and the tropical Atlantic SST EOF1, the tropical North Atlantic SST, and the tropical

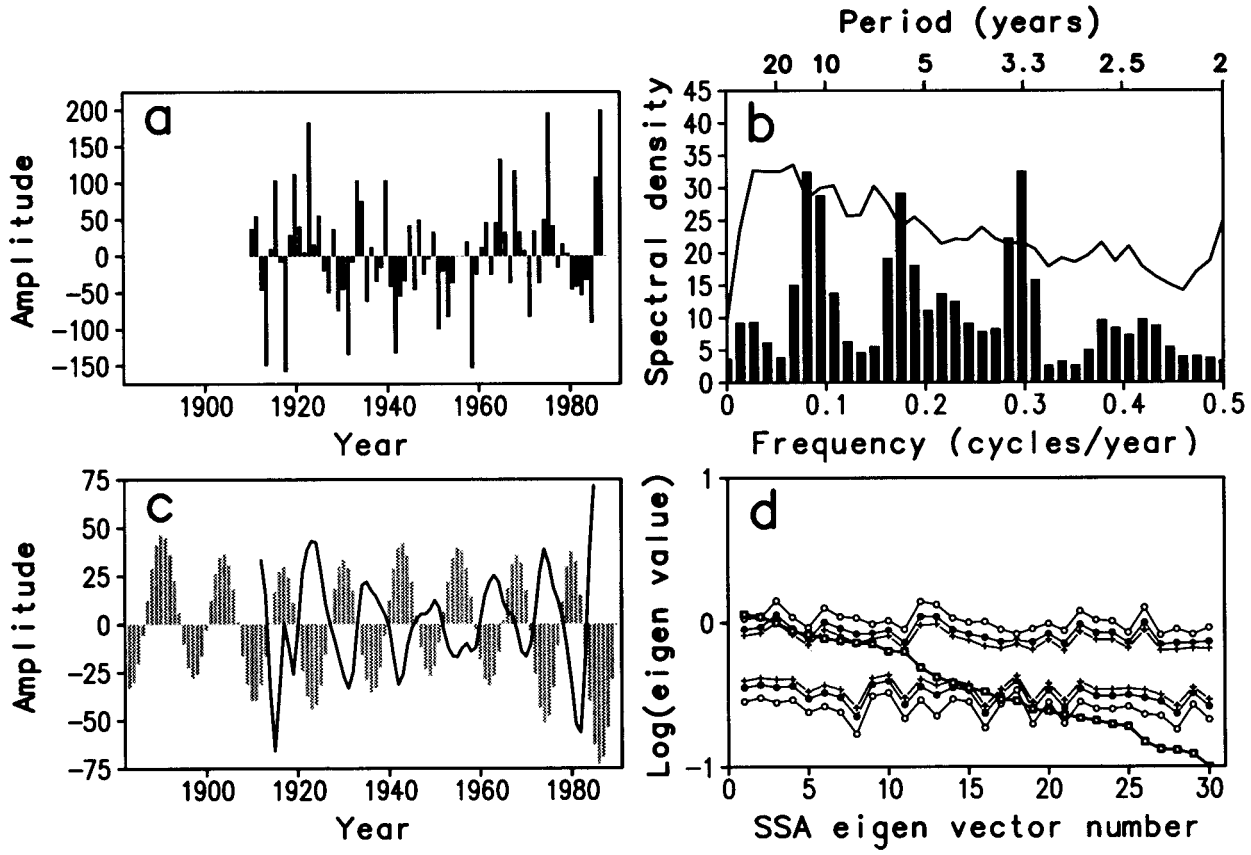

FIG. 10. (a) Time series and (b) the estimated Fourier spectral density of the north Nordeste Brazil rainfall anomalies. The line in (b) shows the 95% confidence level obtained with the Monte Carlo technique. (d) SSA eigenvalue spectrum (box) and the 99%–1% (open circle), 95%–5% (dot), and 90%–10% (cross) Monte Carlo confidence limits on the SSA eigenvalue spectrum. (c) Reconstructed rainfall time series (line) from the first four SSA components explaining 30% of the total north Nordeste Brazil rainfall variance and reconstructed SST PC1 time series (bars) in Fig. 3f multiplied by 200.

South Atlantic SST confirm these Fourier and SSA results. These three cross-spectra are shown in Fig. 11. The squared coherence between the rainfall and each of the three SST time series is approximately 0.9 at the 12–13-yr period. The phase relationship between the rainfall variability and the SST variability at the 12–13-yr period in all three cases is such that the north Nordeste Brazil rainfall is above normal when the SST in the tropical South Atlantic is above normal or when the SST in the tropical North Atlantic is below normal or when both conditions exist nearly simultaneously. Any of these three conditions is supposed to be responsible (see Hastenrath 1991, and references therein) for southward displacement of the intertropical convergence zone (ITCZ) resulting in above normal rainfall over north Nordeste Brazil. As discussed earlier, however, coherent decadal oscillations in the cross-equatorial SST gradient were largely caused by coherent decadal oscillations in the tropical South Atlantic SSTs. Therefore, decadal oscillations in the north Nordeste Brazil rainfall were the result of quasi-periodic north–south displacements of the ITCZ caused by decadal oscillations in the tropical South Atlantic SSTs.

b. The tropical Atlantic cyclone activity

The time series of the NTC index, described briefly in section 3c, between 1886 and 1991 (Fig. 12a) shows decadal–multidecadal variations. The estimated Fourier spectrum of the NTC index (Fig. 12b) has significant peaks at approximately 5–6 yr and 3–4 yr. The spectrum also has other peaks, substantial but below the 95% significance level, at approximately 8–9 yr, 40–50 yr, and 2–3 yr. The SSA eigenvalue spectrum of the NTC index time series is shown in Fig. 12d. The time series reconstructed from the sixth and seventh SSA T-EOFs and T-PCs, explaining 14% variance, has oscillations at near-decadal periods and is shown in Fig. 12c. SSA did not reveal oscillations at similar periods in any SST anomaly time series, but FSA of the SST anomaly time series at 15°N–35°W (Fig. 2d) did show a peak at 8–9 yr. Fourier cross-spectra (not shown) showed approxi-

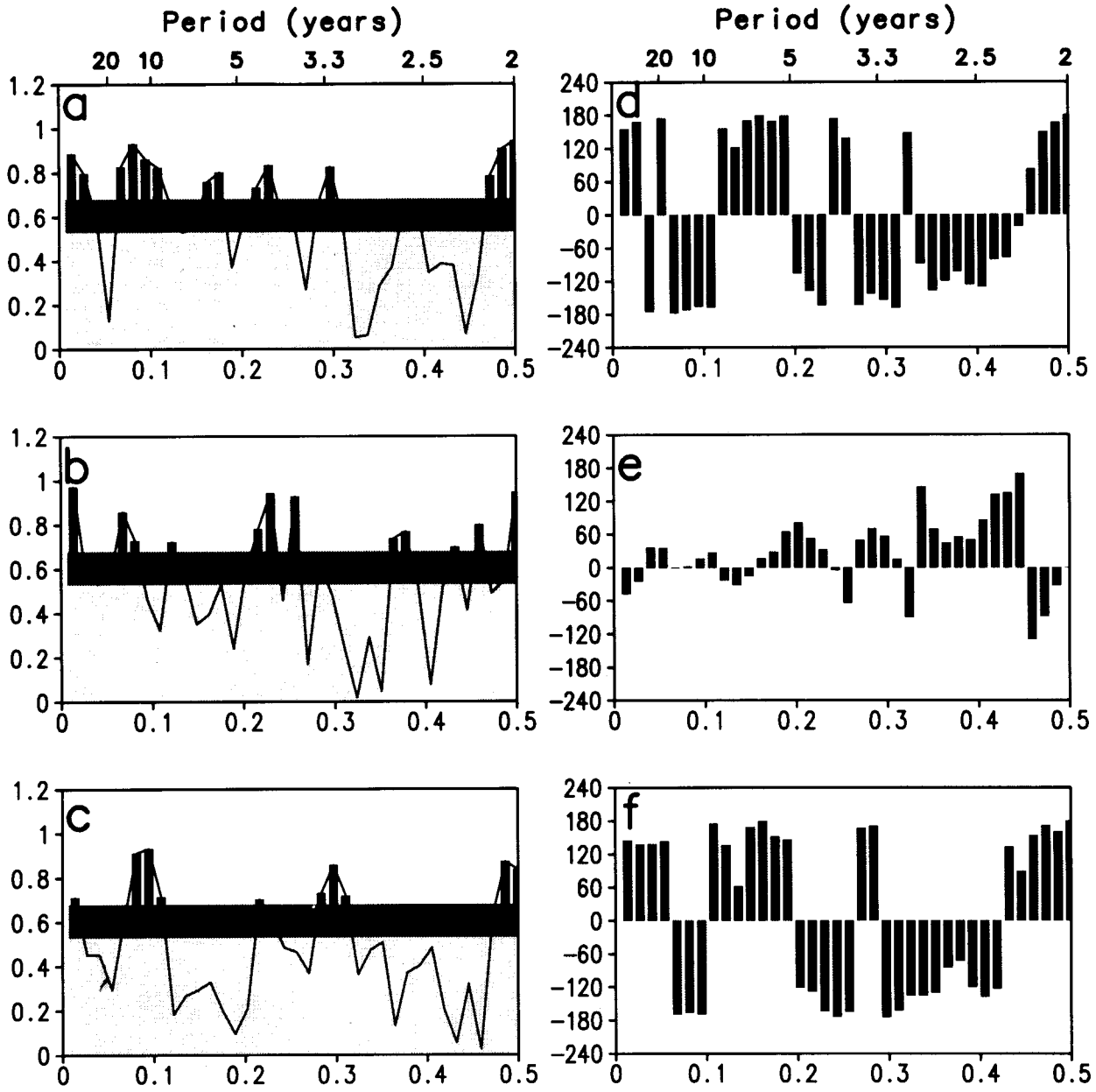

FIG. 11. Squared coherence and phase difference, respectively, between the north Nordeste Brazil rainfall anomalies and (a)–(d) the SST PC1 anomalies, (b)–(e) the SST anomalies at 15°S, 5°E, and (c)–(f) the SST anomalies 15°N, 35°W. In (a), (b), and (c), the solid line is the estimated squared coherence, the lighter shading is the 95% significance level, the darker shading is the 99% significance level, and the black bars denote the squared-coherence that exceeds the 99% level. In (d), (e), and (f), bars denote phase difference.

mately 0.6 squared-coherence with nearly zero phase difference between the NTC index time series and SST anomaly time series in the tropical North Atlantic at near-decadal timescales. Although this squared-coherence exceeds 95% confidence level and the phase difference is physically consistent, it is not very high and, in the absence of corroborative evidence from SSA, should be considered suggestive rather than definitive.

The occurrence of individual variability, and possible covariability between the NTC index and the tropical North Atlantic SST at approximately the same periods, suggests that the two variabilities may be physically related to each other. Even though the decadal SST perturbations are small in amplitude, they cover almost the entire tropical North Atlantic with anomalies of the same sign. Therefore, they may be able to influence tropical cyclone activity by slowly increasing the amount of tropospheric moisture and/or slowly destabilizing the lower troposphere when the SST anomalies are warmer than normal.

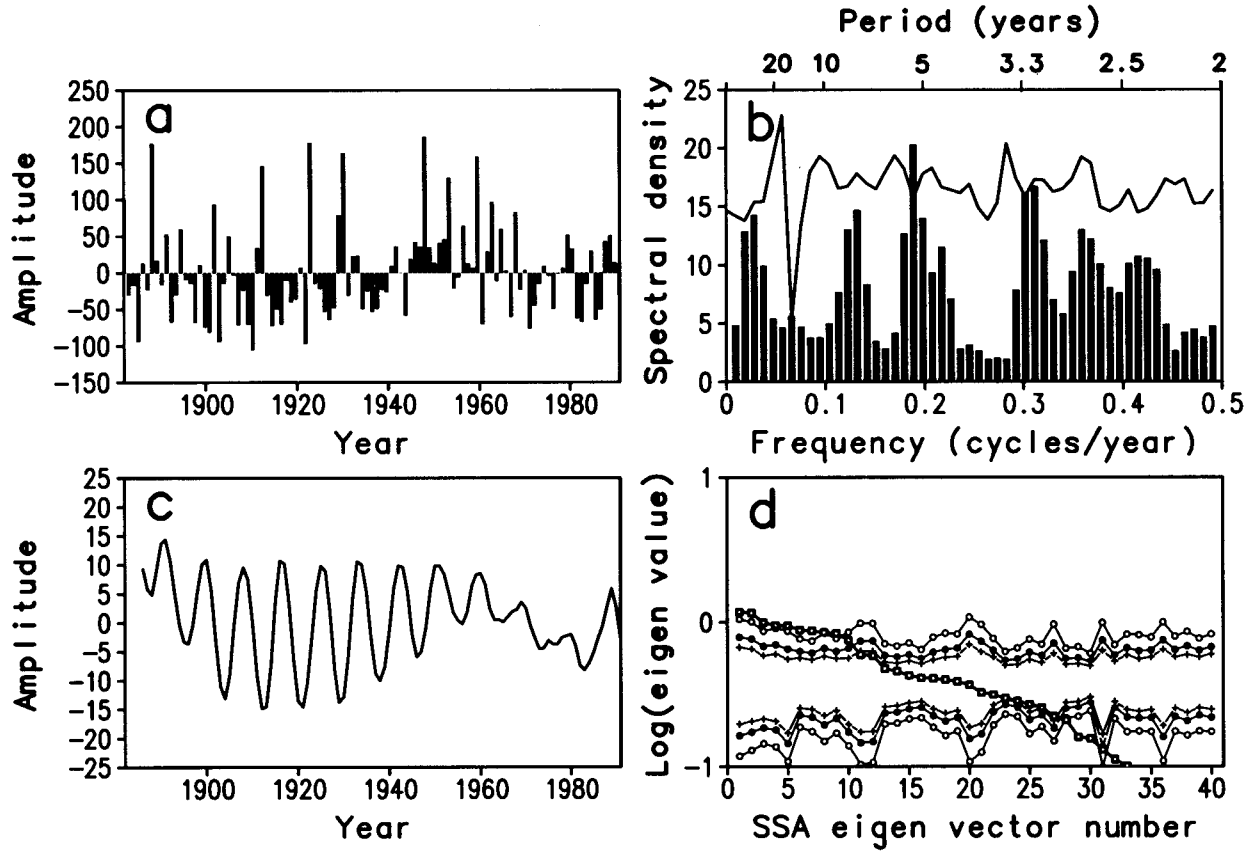

FIG. 12. (a) Time series and (b) the estimated Fourier spectral density of the tropical Atlantic cyclone index. The line in (b) shows the 95% confidence level obtained with the Monte Carlo technique. (d) SSA eigenvalue spectrum (box) and the 99%–1% (open circle), 95%–5% (dot), and 90%–10% (cross) Monte Carlo confidence limits on the SSA eigenvalue spectrum. (c) Reconstructed cyclone index time series (line) from the sixth and seventh SSA components explaining 14% of the total cyclone index variance.

The squared-coherence between the NTC index, and the SST PC1, and the tropical South Atlantic SST anomalies is low. This suggests that oscillations in north–south SST gradient and the resultant north–south displacements in the ITCZ location may not be very important in modulating the Atlantic cyclone activity.

7. Concluding remarks

The questions addressed to the 110-yr-long (1882–1991) tropical Atlantic SST time series, the 74-yr-long (1912–85) north Nordeste Brazil rainfall time series, and the 106-yr-long (1886–1991) tropical Atlantic cyclone index time series were mentioned in the review of previous work. Various analyses of the datasets, described in the preceding sections, have provided answers to these questions.

1) Are there distinct decadal periods at which the tropical Atlantic SSTs oscillate?

   The Fourier, singular, and wavelet spectrum analyses of the tropical Atlantic SST time series in each 10° lat × 10° long grid box and of the tropical Atlantic SST PC1 time series revealed 12–13 yr as the dominant or distinct period of variations in the tropical South Atlantic SSTs and PC1. There are peaks in the Fourier spectra of the tropical North Atlantic SST time series at 8–9 yr, but these peaks do not have high statistical significance and other spectral analyses also do not show a distinct decadal timescale.

2) Are there large-scale, spatially coherent structures of the tropical Atlantic SST anomalies that oscillate at decadal periods?

   Two, possibly physical, modes of decadal SST variations were identified in the tropical North Atlantic. In the more energetic mode, SST anomalies traveled into the tropical North Atlantic from the extratropical North Atlantic along the eastern boundary of the basin. The anomalies then frequently traveled through the tropical North Atlantic from east to west, then into the mid-high latitudes along the western boundary of the basin, and completed a clockwise rotation around the North Atlantic basin. In the less energetic mode, SST anomalies appeared to originate in the tropical–subtropical Atlantic near the African coast, and traveled northwestward and

southward. There was no distinct decadal timescale of variation of these modes and there were multidecadal modulations of their amplitudes. Active epochs of these modes were episodic. In a possibly physical mode in the South Atlantic, anomalies arrived from the subtropics, frequently traveled through the tropical South Atlantic from east to west, then into the subtropical latitudes along the western boundary of the basin, and completed a counterclockwise rotation around the South Atlantic basin. These rotations/oscillations in the South Atlantic were completed in 12–13 yr. Both the tropical North and South Atlantic SST anomalies frequently crossed the equator and, because they resided in the tropical Atlantic for several years, created the appearance of a dipole SST pattern straddling the equator. It was shown that variations in this statistical SST dipole pattern can be interpreted as the cross-equatorial SST gradient variations.

The detailed analysis and identification of several types of decadal SST variations in the tropical Atlantic in this study confirms the preliminary results in MD.

3) Is there a definite relationship between the tropical Atlantic and mid–high-latitude Atlantic decadal variabilities?

   As described in 2), incursions of extratropical SST anomalies into the tropical Atlantic along the eastern boundaries occurred in both hemispheres. Statistically, however, low (0.1–0.4) squared-coherence between the tropical and midlatitude North Atlantic SST variations at decadal periods was found. Perhaps, this was due to the absence of a distinct decadal timescale in the North Atlantic SST variations. The squared-coherence increased to 0.6 at high latitudes with a few years phase difference suggesting that there may be a connection between the tropical and high-latitude Atlantic SST variations.

4) Is there covariability among the SSTs, the north Nordeste Brazil rainfall, and the tropical Atlantic cyclone index at decadal periods?

   Independent analyses of rainfall over north Nordeste Brazil revealed a significant spectral peak at the 12–13-yr period indicated by previous analyses. The Fourier cross-spectrum between the rainfall and the tropical Atlantic SST time series revealed a peaked and significant squared-coherence (0.9) between the rainfall variations and variations of the cross-equatorial SST gradient pattern at the 12–13-yr period. The cross-equatorial SST gradient and the rainfall time series have decadal, high-variance, SSA eigenmodes that are physically consistent. The estimated spectra of the tropical Atlantic cyclone index time series and the tropical North Atlantic SST time series have a peak at approximately 8–9-yr period. The Fourier cross-spectrum between the cyclone index and the tropical North Atlantic SST time series also has a peaked squared-coherence (0.65) at the 8–9-yr period, with the phase difference such that cyclone activity lags warmer SSTs by a few years. Since the spectral and cross-spectral results do not have high statistical significance, the relationship between the cyclone index and the tropical Atlantic SSTs at decadal timescales is only suggestive. Although multidecadal variations in approximately 100-yr-long time series should not be considered significant, it is interesting to note that the tropical Atlantic SSTs, the north Nordeste Brazil rainfall, and the tropical Atlantic cyclone index exhibit physically consistent multidecadal (40–50-yr period) variations.

SST measurement techniques have changed several times over the 110-yr analysis period. These changes and the general concerns about any SST measurements before the Second World War would introduce significant doubts in the credibility of results obtained with the analyses of such long time series. The apparent physical agreement among the decadal variations in the tropical Atlantic SSTs, the independently measured north Nordeste Brazil rainfall, and the tropical Atlantic cyclone index significantly enhances the credibility of the results. The internal consistency of independent analyses of SST anomalies in neighboring grid boxes also makes the results more credible, although systematic errors in SST measurements over the whole domain can also give similar results in all grid boxes.

The results of this study have enabled us to identify important features of the tropical Atlantic decadal variations that a comprehensive theory will have to explain. These features are (i) a preference for the 12–13-yr oscillation period in the tropical South Atlantic and the absence of a distinct decadal period in the tropical North Atlantic, (ii) rotations of SST anomalies around the North and South Atlantic, (iii) locations of the largest tropical SST anomalies at approximately 15°N and 15°S, and weaker SST anomalies near the equator, (iv) cross-equatorial travel of SST anomalies, and (v) relationship between decadal and multidecadal variations. The results also show that the dipole pattern of SST variations revealed by empirical orthogonal function analyses of SST anomalies should be interpreted as variations in the cross-equatorial SST gradient associated with the decadal variations identified in the present study. Approximately 80% of the coherent decadal variance in the cross-equatorial SST gradient was explained by coherent decadal oscillations in the tropical South Atlantic SSTs during the analysis period. These results are clearly inconsistent with the paradigm of unstable tropical Atlantic ocean–atmosphere interactions resulting in a cross-equatorial, dipole mode of tropical Atlantic SST variations at decadal timescales. The initial interpretation of preliminary results from the Geophysical Fluid Dynamics Laboratory coupled ocean–atmosphere model by MD, and the modeling study by Chang et al. (1997) were based on this paradigm. The results of the present study suggest an alternate paradigm of the tropical At-

lantic decadal SST variations in which Tropics–extratropics interactions via the ocean and the atmosphere may be very important. The role of the tropical Atlantic ocean–atmosphere interactions in this alternate paradigm is not clear from the present study.

The results of the present study show that the climate of the tropical Atlantic and some neighboring continental regions has undergone quasi-regular oscillations at decadal timescales during the 110-yr analysis period. The rainfall variability affects water resources and agriculture in Brazil, and the variability in cyclone activity affects the United States, Mexico, and the Caribbean countries. The societal impacts of these quasi-regular decadal oscillations can be mitigated/exploited if the decadal climate anomalies can be predicted in advance. The quasi-regularity suggests that the decadal climate anomalies may be predictable with some accuracy several years in advance. Therefore, the study of the tropical Atlantic decadal climate variability and its predictability should be one of the foci of the Climate Variability and Predictability Program organized by the World Climate Research Program.

Acknowledgments. The author is grateful to V. K. Dubey for his help in data analysis and to W. Gray for the use of the tropical Atlantic cyclone activity index time series. The author is also grateful to A. Busalacchi, T. Delworth, C. Folland, Inez Fung, S. Hastenrath, R. Houghton, M. Latif, S. Levitus, S. Zebiak, and two anonymous reviewers for carefully reading earlier versions of the manuscript and making useful suggestions. Discussions with T. N. Krishnamurti about the physical relationship between SST and hurricane activity, and with R. Cahalan about EOFs and physical modes of variability are thankfully acknowledged. The author expresses his deep appreciation to K.-M. Lau for supporting this work and to Ms. Laura Rumburg for drafting the illustrations. This work was partially supported by NOAA Grant NA93AANAGO349.

REFERENCES

Allen, M. R., and L. A. Smith, 1994: Investigating the origins and significance of low-frequency modes of climate variability. *Geophys. Res. Lett.,* **21,** 883–886.

Barnett, T. P., 1983: Interaction of the monsoon and Pacific trade wind system at interannual time scales. Part I: The equatorial zone. *Mon. Wea. Rev.,* **111,** 756–773.

Bloomfield, P., 1976: *Fourier Analysis of Time Series: An Introduction.* John Wiley and Sons, 258 pp.

Bottomley, M., C. K. Folland, J. Hsiung, R. E. Newell, and D. E. Parker, 1990: *Global Ocean Surface Temperature Atlas (GOSTA).* Her Majesty's Stationery Office.

Broomhead, D. S., and G. King, 1986: Extracting qualitative dynamics from experimental data. *Physica D,* **20,** 217–236.

Brunet, G., and R. Vautard, 1996: Empirical normal modes versus empirical orthogonal functions for statistical prediction. *J. Atmos. Sci.,* **53,** 3468–3489.

Burg, J. P., 1978: Maximum entropy spectral analysis. *Modern Spectrum Analysis,* D. G. Childers, Ed., IEEE Press, 34–41.

Chang, P., L. Ji, and H. Li, 1997: A decadal climate variation in the tropical Atlantic Ocean from thermodynamic air–sea interactions. *Nature,* **385,** 516–518.

Deser, C., and M. L. Blackmon, 1993: Surface climate variations over the North Atlantic during winter: 1900–1989. *J. Climate,* **6,** 1743–1753.

Enfield, D. B., and D. A. Mayer, 1997: Tropical Atlantic sea surface temperature variability and its relationship to El Niño–Southern Oscillation. *J. Geophys. Res.,* **102,** 929–945.

Folland, C. K., T. N. Palmer, and D. E. Parker, 1986: Sahel rainfall and worldwide sea temperatures. *Nature,* **320,** 602–606.

——, J. A. Owen, M. N. Ward, and A. W. Colman, 1991: Prediction of seasonal rainfall in the Sahel region using empirical and dynamical methods. *J. Forecasting,* **10,** 21–56.

——, R. W. Reynolds, M. Gordon, and D. E. Parker, 1993: A study of six operational sea surface temperature analyses. *J. Climate,* **6,** 96–113.

Gray, W. M., C. W. Landsea, P. W. Mielke Jr., and K. J. Berry, 1992: Predicting Atlantic seasonal hurricane activity 6–11 months in advance. *Wea. Forecasting,* **7,** 440–455.

——, ——, ——, and ——, 1994: Predicting Atlantic basin seasonal tropical cyclone activity by 1 June. *Wea. Forecasting,* **9,** 103–115.

Gu, D., and S. G. H. Philander, 1995: Secular changes of annual and interannual variability in the Tropics during the past century. *J. Climate,* **8,** 864–876.

Hastenrath, S., 1990: Decadal-scale changes of the circulation in the tropical Atlantic sector associated with Sahel drought. *Int. J. Climatol.,* **10,** 459–472.

——, 1991: *Climate Dynamics of the Tropics.* Kluwer Academic Publishers, 488 pp.

——, M.-C. Wu, and P.-S. Chu, 1984: Towards the monitoring and prediction of north-east Brazil droughts. *Quart. J. Roy. Meteor. Soc.,* **110,** 411–425.

Horel, J. D., 1981: A rotated principal component analysis of the interannual variability of the Northern Hemisphere 500 mb height field. *Mon. Wea. Rev.,* **109,** 2080–2092.

——, 1984: Complex principal component analysis: Theory and examples. *J. Climate Appl. Meteor.,* **23,** 1660–1673.

Houghton, R. W., and Y. M. Tourre, 1992: Characteristics of low frequency sea surface temperature fluctuations in the tropical Atlantic. *J. Climate,* **5,** 765–771.

Kawamura, R., 1994: A rotated EOF analysis of global sea surface temperature variability with interannual and interdecadal scales. *J. Phys. Oceanogr.,* **24,** 707–715.

Landsea, C. W., 1993: A climatology of intense (or major) Atlantic hurricanes. *Mon. Wea. Rev.,* **121,** 1703–1713.

Lau, K.-M., and H. Weng, 1995: Climate signal detection using wavelet transform: How to make a time series sing. *Bull. Amer. Meteor. Soc.,* **76,** 2391–2402.

Mehta, V. M., and T. Delworth, 1995: Decadal variability of the tropical Atlantic Ocean surface temperature in shipboard measurements and in a global ocean–atmosphere model. *J. Climate,* **8,** 172–190.

Meyers, S. D., B. G. Kelly, and J. J. O'Brien, 1993: An introduction to wavelet analysis in oceanography and meteorology: With application to the dispersion of Yanai waves. *Mon. Wea. Rev.,* **121,** 2858–2866.

Nobre, P., and J. Shukla, 1996: Variations of sea surface temperature, wind stress, and rainfall over the tropical Atlantic and South America. *J. Climate,* **9,** 2464–2479.

North, G. R., 1984: Empirical orthogonal functions and normal modes. *J. Atmos. Sci.,* **41,** 879–887.

——, T. L. Bell, R. F. Cahalan, and F. J. Moeng, 1982: Sampling errors in the estimation of empirical orthogonal functions. *Mon. Wea. Rev.,* **110,** 75–82.

Parker, D. E., P. D. Jones, C. K. Folland, and A. Bevan, 1994: Interdecadal changes of surface temperature since the late nineteenth century. *J. Geophys. Res.,* **99,** 14 373–14 399.

Penland, C., M. Ghil, and K. M. Weickmann, 1991: Adaptive filtering and maximum entropy spectra with application to changes in atmospheric angular momentum. *J. Geophys. Res.,* **96,** 22 659–22 671.

Press, W. H., B. P. Flannery, S. A. Teukolsky, and W. T. Vetterling, 1987:

Numerical Recipes: The Art of Scientific Computing. Cambridge University Press, 818 pp.

Rasmusson, E. M., P. A. Arkin, W. Y. Chen, and J. B. Jalickee, 1981: Biennial variations in surface temperature over the United States as revealed by singular decomposition. *Mon. Wea. Rev.,* **109,** 181–192.

Semazzi, F. H. M., V. M. Mehta, and Y. C. Sud, 1988: An investigation of the relationship between sub-Saharan rainfall and global sea surface temperatures. *Atmos.–Ocean,* **26,** 118–138.

Ulrych, T. J., and T. N. Bishop, 1975: Maximum entropy spectrum analysis and autoregressive decomposition. *Rev. Geophys. Space Phys.,* **13,** 183–200.

Vautard, R., and M. Ghil, 1989: Singular spectrum analysis in nonlinear dynamics with applications to paleoclimatic time series. *Physica D,* **35,** 395–424.

Ward, M. N., and C. K. Folland, 1991: Prediction of seasonal rainfall in the north Nordeste of Brazil using eigenvectors of sea-surface temperature. *Int. J. Climatol.,* **11,** 711–743.